

JPRS-JST-92-023  
22 SEPTEMBER 1992



FOREIGN  
BROADCAST  
INFORMATION  
SERVICE

# ***JPRS Report***

## **Science & Technology**

***Japan***

**DISTRIBUTION STATEMENT A**

Approved for public release;  
Distribution Unlimited

**FIFTH SYMPOSIUM ON ULTRAHIGH  
TEMPERATURE MATERIALS**

19980113 378

**DTIC QUALITY INSPECTED 3**

REPRODUCED BY  
U.S. DEPARTMENT OF COMMERCE  
NATIONAL TECHNICAL INFORMATION SERVICE  
SPRINGFIELD, VA 22161

JPRS-JST-92-023  
22 SEPTEMBER 1992

SCIENCE & TECHNOLOGY  
JAPAN

FIFTH SYMPOSIUM ON ULTRAHIGH  
TEMPERATURE MATERIALS

926C0064 Ube CHO KO' ON ZAIRYO SYMPOSIUM in Japanese 12-13 Mar 92 pp 1-93

[Selected papers from the Fifth Symposium on Ultrahigh Temperature Materials—Properties and Applications held 12-13 Mar 92 in Ube City, sponsored by Yamaguchi Prefectural Government, JUTEM, JUTEMI, et al.]

CONTENTS

Superplastic Forming of Ceramics at Elevated Temperatures [Fumihiro Wakai].....	1
Properties, Applications of Zirconia Ultrahigh Temperature Material [Hajime Asami].....	9
Plasmas, Related High-Temperature Materials [Osamu Fukumasa].....	22
Some Problems of Technology Advanced Structural Materials Testing, Evaluation at Ultrahigh Temperature [Kazumi Hirano].....	29

## **Superplastic Forming of Ceramics at Elevated Temperatures**

926C0064A Ube CHO KO' ON ZAIRYO SYMPOSIUM in Japanese 12-13 Mar 92 pp 34-40

[Article by Fumihiro Wakai: "Superplasticity of Ceramics; Quantitative Descriptions and Models of Superplastic Characteristics; Damage and Fracture by Superplastic Deformation; Applications to Superplastic Processing"]

[Excerpts] **Abstract:** Superplastic forming of ceramics had been, for a long time, a dream of material scientists and engineers who believed in the achievement of deformation processing for ceramics. Now it is a reality and the technological horizon in superplastic ceramics is gradually expanding. Numerous works on superplasticity of  $ZrO_2$  ceramics since 1985 revealed some characteristics of superplasticity, microstructural feature, and possible mechanisms. Recent advances in ceramic processing brought about not only superplastic structural ceramics ( $ZrO_2$ ,  $Al_2O_3$ , mullite,  $Si_3N_4$ , SiC, and their composites), but also superplastic functional ceramics that have characteristic properties such as electronic, magnetic, optical, chemical, or biological properties. The phenomenon can be used in superplastic forming, solid-state bonding, sinter-forging, hot press, and hot-isostatic pressing. A recent demonstration of blow forming of a ceramic composite sheet clearly indicates that superplastic forming of ceramics is applicable to the aerospace industry.

### **3. Superplasticity of Plastics**

#### **3.1 Crystal Grains Refining Technology**

Grain size of 1  $\mu m$  or below is the requirement for the manifestation of superplasticity. The key to obtaining refined crystal grains of ceramics manufactured by the powder metallurgy method was to develop ultrafine particles and starter powders with a free degree of sintering. Methods for manufacturing fine particles include the coprecipitation method ( $ZrO_2$ ), precursor method ( $Al_2O_3$ ), sol-gel method (mullite), alkoxide method (oxide superconductors), chemical vapor deposition (CVD) method ( $Si_3N_4/SiC$  composite material), and wet method (hydroxyapatite). In order to prevent crystal grain size of sintered bodies from becoming bulky, sintered bodies must be compacted at low temperatures. Control of grain growth, addition of sintering assistants to promote making grains closer, and pressure sintering, such as hot press and hot isostatic pressing (HIP) are effective to this end.

### 3.2 Expansion in Material System

A superplastic phenomenon has resulted in a new potential in applications of many ceramics with useful properties. Table 1 is a summary of ceramics functions and examples of their applications. Their superplasticity and high ductility were demonstrated by the underlined materials. With structural ceramics (Y-TZP,  $\text{Al}_2\text{O}_3$ , mullite,  $\text{Si}_3\text{N}_4$ , and  $\text{SiC}$ ) and their composite materials, an attempt has already been made of near net shape molding of mechanical parts by superplastic machining. Superplasticity of functional ceramics has been found only recently. The majority of electronic ceramics are perovskite-type crystals, while  $\text{PbTiO}_3$ , a piezoelectric ceramics, for example, showed the elongation in superplasticity. The improvement in superplasticity of oxide superconductive materials is being promoted by Kodama, et al.  $\text{ZrO}_2$ , in which superplasticity was first discovered, is a good oxygen ion conductor, used as a solid electrolyte. Furthermore, the superplasticity of hydroxyapatite, "bioceramics," was also reported. The current status of superplasticity of ceramics is summarized in the literature [not reproduced].

Table 1. Applications of Ceramics

Field	Function	Materials	Device
Mechanical properties	Strength	$\text{Si}_3\text{N}_4$ , $\text{SiC}$ $\text{ZrO}_2$ , Mullite, $\text{Al}_2\text{O}_3$	Components for engine
Electronic properties	Dielectric Piezoelectric Pyroelectric  Insulation Semiconductive Superconductive  Ionic conductive	$\text{BaTiO}_3$ $\text{PZT}$ , $\text{PbTiO}_3$ $\text{PZT}$  $\text{Al}_2\text{O}_3$ $\text{BaTiO}_3$ $\text{YBa}_2\text{Cu}_3\text{O}_{7-x}$ , $\text{Bi}_2\text{Sr}_2\text{Ca}_2\text{Cu}_3\text{O}_{10}$ $\text{ZrO}_2$	Capacitor Transducer Infrared ray sensor IC substrate Thermistor Electric cable  Fuel cell, oxygen sensor
Magnetic properties	Ferromagnetic (Soft) (Hard)	$\text{Zn}_{1-x}\text{Mn}_x\text{Fe}_2\text{O}_4$ $\text{SrO-6Fe}_2\text{O}_3$	Magnetic head Magnet
Optical properties	Transparent Electrooptic	$\text{ZnS}$ $\text{PLZT}$	Laser window Optical switch
Biological properties	Bioactive Bioinert	Hydroxyapatite $\text{Al}_2\text{O}_3$ , $\text{ZrO}_2$	Artificial bone

## 4. Quantitative Descriptions of Superplastic Characteristics and Their Models

### 4.1 Superplastic Deformation and Local Necking

The development of necking must be controlled for homogeneous elongation of a specimen as the one in Figure 2 to be possible. Supposing that it is possible to express the deformation of a continuous body as  $\sigma = A\dot{\epsilon}^m \exp(\gamma\epsilon)$  ( $\sigma$ , stress;  $\dot{\epsilon}$ , rate of strain;  $\epsilon$ , strain;  $m$ , sensitivity index or rate of strain;  $\gamma$ , strain hardening time), the condition for homogeneous deformation can be determined by the relationship between the value of  $m$  and  $\gamma$  from dynamic analysis of plastic stability. The value of  $m$  of superplastic ceramics is 0.5, equivalent to that of many other superplastic alloys.

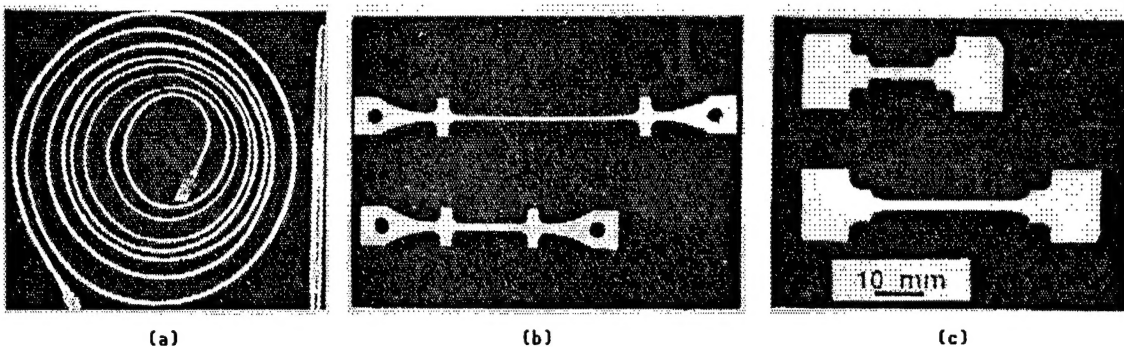


Figure 2. Superplasticity of Polycrystalline Solids

- (a) Metals, Sn-Bi alloy
- (b) Ionic crystals, Y-TZP
- (c) Covalent polycrystals,  $\text{Si}_3\text{N}_4/\text{SiC}$  composite

### 4.2 Superplastic Characteristics

The deformation characteristics of Y-TZP, which is regarded as a standard superplastic ceramic, were analyzed from stress-strain curves in tensile and compression tests and creep tests. The structural equation for the superplastic deformation is as follows:

$$\dot{\epsilon} = K(b/d)^p (\sigma/G)^n D_0 \exp(-Q/RT) \quad (1)$$

where  $b$ ,  $d$ ,  $p$ ,  $G$ ,  $n$ ,  $D_0 \exp(-Q/RT)$ ,  $Q$ ,  $R$ , and  $T$  represent baggase vector, grain size, grain size dependency index, rigidity, stress index ( $n=1/m$ ), diffusion coefficient, activated energy, gas constant, and absolute temperature, respectively.

A thorough investigation was made by researchers on the influence of the rate of strain, temperatures, grain size, crystal phase, solution ion concentration, composition, and quantity of trace impurities and intergranular structure on fluidized stress and fracture elongation, and the parameters in equation (1) were determined. Figure 3 shows the influence of grain size on the rate of strain.

#### 4.3 Superplasticity Deformation Models

It is clear by a study of post deformation particulate aspect ratios that with superplastic ceramics, intergranular slip greatly contributes to their total deformation.

As an intergranular slip model of superplasticity, the geometric model based on the rearrangement of crystal grains (particulate switching) by Ashby and Verral is a classic. It is a mass transfer rate in the neighborhood of the grain boundary that rate-determines the deformation by intergranular slip.

Two mechanisms are related in series to the transport process by dispersion mechanisms—interfacial reactions of the generation and dissipation of holes and the diffusion process in the grain boundary. If one supposes that intergranular slip rate-determined by interfacial reactions (stress index, 2) is a superplastic mechanism of a fine particle material and that every grain boundary rate-determined by diffusion acts in series, the stress index dependency on the grain size can be explained. Furthermore, it was interpreted that the rate of strain of a superplastic material was lower than the intergranular diffusion creep rate because it was rate-determined by intergranular reactions.

#### 4.4 Superplasticity With High Rate of Strain by Intergranular Engineering

Decreased processing temperature and improved processing speed are demanded for the practical use of superplastic processing. To improve workability, refining crystal grains and controlling intergranular structure are effective. The segregation of impurities to the grain boundary and the existence of a liquid phase in it affect intergranular dispersion or an interfacial reaction rate, thereby promoting superplastic deformation.

The influence of trace impurities on superplastic deformation was first pointed out by Nauer, et al., while Hermansson, et al., investigated the relationship between the quantity of an amorphous phase and deformation properties. Yoshizawa, et al., investigated the effect of the chemical composition of an amorphous intergranular phase (5 wt%) and reported that lithium silicate glass is most effective to lower deformation temperatures.

The institute found that high-speed deformation of Y-TZP was enabled by adding a trace quantity of a transition metal. Y-TZP to which 0.3 mol% Mn was added, for example, was refined at 1300°C, resulting in its grain size of 0.27  $\mu\text{m}$ . Superplastic deformation was promoted by adding Mn with the result that, for example, two-fold elongation at 1450°C required only 50 seconds. Superplastic

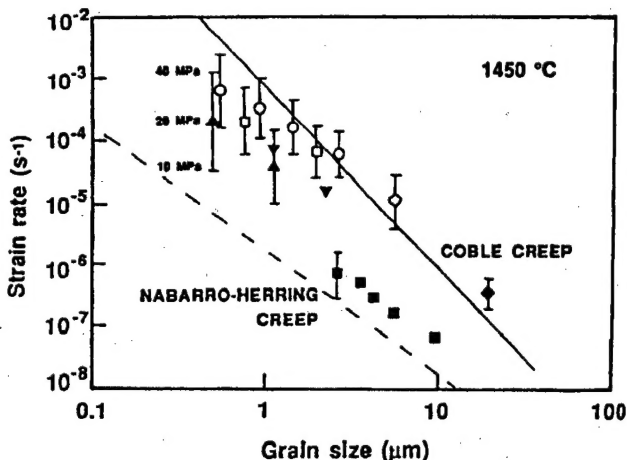


Figure 3. Relationship Between Strain Rate and Grain Size of  $\text{ZrO}_2$  Polycrystals at 1450°C and 20 MPa

deformation was also possible at 1250°C. With CuO-added Y-TZP, a liquid phase was formed in the grain boundary to promote superplastic deformation.

#### **4.5 Superplasticity of Composite Materials**

Deformation behavior of a two-phase composite material changes from a single-phase material behavior because of the diffusion of second-phase particles. The deformation of a system that regards that "hard" or "soft" second-phase particles are homogeneously diffused in the base phase that undergoes superplastic deformation can be described with a rheology model. The deformation of a composite material in which second-phase particles are diffused is basically controlled by fluid properties of the base phase. For example, it is known that a rheology model holds for superplastic deformation of a zirconia/alumina composite material and a zirconia/mullite composite material. Based on this model, assuming that certain ceramics show superplasticity, a composite material obtained by diffusing other second-phase particles in the ceramics also shows superplasticity.

### **5. Damage and Fracture by Superplastic Deformation**

#### **5.1 Formation and Growth of Cavities**

Cavities are formed during superplastic deformation in many alloys and ceramics. Cavities are formed in grain boundaries because of inner defects or an insufficient adjustment mechanism in intergranular slip. Fracture of a superplastic material can be divided into four processes: 1) the formation of cavity nuclei, 2) cavity growth, 3) connection, and 4) crack propagation. Cavities remaining in superplastic processing materials cause strength to deteriorate.

Cavity growth rates and dimensional distribution in superplastic ceramics were quantitatively investigated as functions of temperature, the rate of strain, and strain. Cavity volume rapidly increases in the neighborhood of fracture strain, while it is clear that it is negligible below certain strain without affecting strength.

#### **5.2 Fracture by Creep Crack Growth**

It was shown that a power multiplication law holds between the crack growth rate and fluid stress. It has been able to predict optimum test conditions for obtaining fracture elongation and maximum elongation under a given test condition by linking the above law with a compositional equation for superplastic deformation.

### **6. Applications to Superplastic Processing**

Ceramics parts are manufactured through the processes of 1) material preparation, 2) forming, 3) sintering, and 4) processing. Plastic deformation of ceramics at high temperatures is used for pressure sintering and hot forming shown in Figure 4.

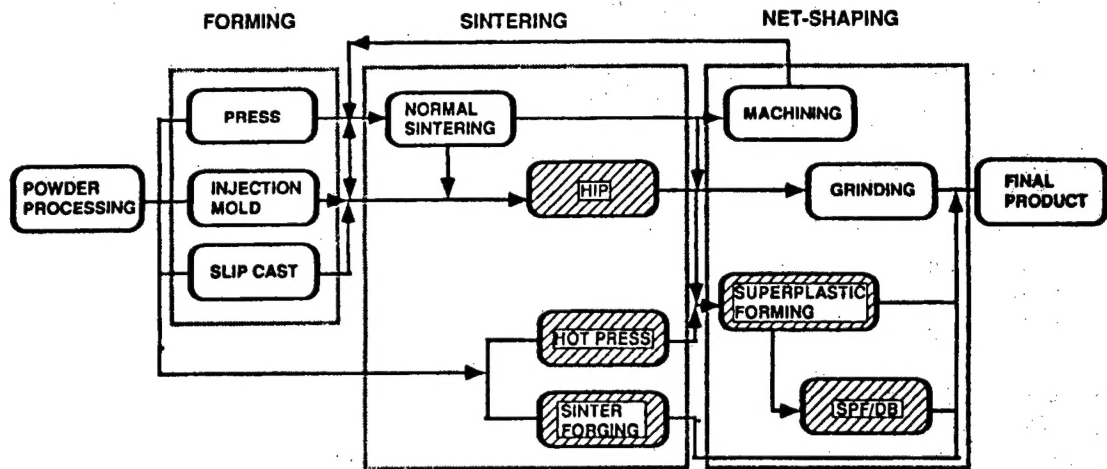


Figure 4. Stress-Assisted Densification Process and Hot-Forming Process in the Fabrication of Ceramic Components

### 6.1 Near-Net-Shape Forming

Superplastic ceramics can be formed at relatively low stress and temperatures. Their close sintered bodies enable free forming providing high-dimensional precision and good finished surface roughness, thus permitting near-net-shape forming. In the case of deformation by compressive stress as is with forging, inner holes and cracks dissipate and strength improves.

In superplastic forging requiring a large sum of funds to be invested in expensive processing materials and processing equipment, a simulation is carried out to determine shapes of materials and dies and other processing conditions and ensure that the final dimensional precision, and optimum molding conditions are predicted for forging. As the compositional equation for describing the deformation of superplastic ceramics is basically the same as the one for superplastic alloys, the already developed three-dimensional finite-element program for superplastic forging can be used as it is (Figure 5 [not reproduced]).

Figure 6 shows examples of superplastic forming of Y-TZP

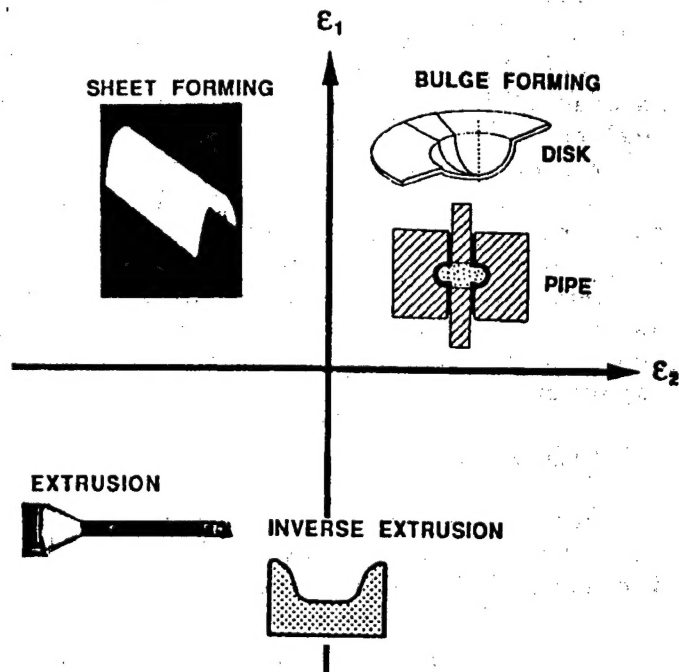


Figure 6. Examples of Superplastic Forming for Y-TZP

published so far. They are easiest to process by compressive stress as in forging, and were processed first. As an example of two-axis compression processing, forward extrusion and backward extrusion of round bars were conducted. Also, Figure 7 [not reproduced] shows an example of thin plate forming of Y-TZP and a jig. Superplastic processing technologies by two-axis tension are most difficult technically, and characteristics of superplastic phenomena have been developed, which include bulge processing of pipes using powder pressure, dome forming by punch testing, and deep drawing. Most recently, a report has been made on processing of hemispherical parts by gas pressure forming (Figure 1 [not reproduced]). Thus, it has been demonstrated that superplastic processing in any multiaxial state theoretically is possible. Gas pressure forming, in particular, requires only half the number of expensive dies and results in great economic advantages, so that these technologies have been established as practical industrial technologies.

Progress in refining crystal grains and intergranular structural control has enabled the superplastic processing temperature of Y-TZP to be lowered to 1150°C and hydroxyapatite to be processed at 1000°C. With transition metal-added Y-TZP, superplastic processing itself can be completed in several seconds.

## 6.2 Applications to Junction

Diffused junction is applied to manufacturing large complex-shaped parts. With titanium alloys difficult to weld, complex-shaped parts are industrially manufactured by performing diffused junction simultaneously with superplastic processing (SPF/DB process). This process is also applicable to superplastic ceramics, and Nagano, et al., published that a junction strength of 1300 MPa could be obtained in superplastic junction of  $ZrO_2/Al_2O_3$  and mullite/ $ZrO_2$  composite materials.

Figure 8 and Figure 9 [not reproduced] show a conceptual drawing of forming of a sandwich structure by the SPF/DB method and an example of blow forming of Ti6Al4V, respectively. It is obvious that a combination of blow forming shown in Figure 1 [not reproduced] and junction enables forming of such a structure to be applied to ceramics materials.

## 6.3 Applications to Pressure Sintering

In pressure sintering processes such as hot press and HIP, such deformation mechanisms as yield, power multiplication law creep, and diffused creep play an important role in refining. In pressure sintering of ultrafine particles, in particular, a superplastic deformation mechanism is also involved in it. Improvement in strength by hot press and IP is conventional wisdom now.

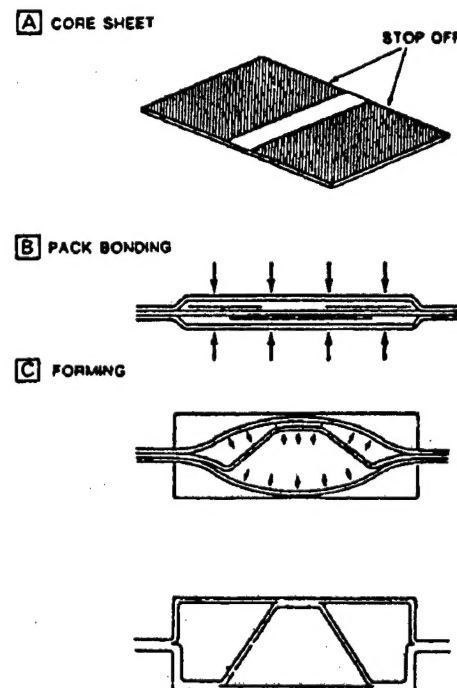


Figure 8. Schematic Illustration of SPF/DB Three-Sheet Fabrication (D. Stephen, 1986)

Sintered forging is near-net-shape forming in which a preform of fine particles was compressed at high temperature, thereby simultaneously providing sintering and deformation. When sintered forging of Y-TZP was conducted at 1,400°C, a preform was completely refined and formed into its final shape in 10 minutes. Also, it was shown that Y-TZP strength could be improved by sintered forging.

## 7. Conclusion

Since the discovery of superplasticity of ceramics, many ceramics materials have been made superplastic, and this phenomenon is being disseminated as technology. Superplastic processing is likely to have a wide range of influence in the ceramics industry in the future, and is expected to make further progress.

## Properties, Applications of Zirconia Ultrahigh Temperature Material

926C0064B Ube CHO KO' ON ZAIRYO SYMPOSIUM in Japanese 12-13 Mar 92 pp 42-51

[Article by Hajime Asami: "Characteristics of Zirconia; Applications of Zirconia; Zirconia Fiber; Zirconia Heating Element"]

**[Excerpts] Abstract:** Zirconia is a unique ceramic raw material having characteristics such as a high melting point (2700°C), low vapor pressure, low thermal conductivity, ion conductivity, excellent chemical resistance, etc.

This paper describes the typical characteristics and applications of zirconia, and also reviews the zirconia fiber and zirconia heating element developed in our laboratory.

### 2. Characteristics of Zirconia

Zirconia is a high fire-resistant material with a high melting point of about 2700°C, possessing the following unique properties.

Zirconia's thermal conductivity shows the smallest value, as shown in Figure 1, compared to those of other oxides, implying that it possesses excellent adiabatic quality without the need to make it porous. Therefore, a zirconia fiber board obtained by forming zirconia in the form of fiber makes a superior heat insulator.

As shown in Figure 2, vapor pressure of zirconia at high temperatures is the lowest compared to those of other oxides. When fine ceramics are sintered in a kiln lined with a zirconia refractory, for example, the lining material has little influence on the heating object, thereby resulting in clean sintering.

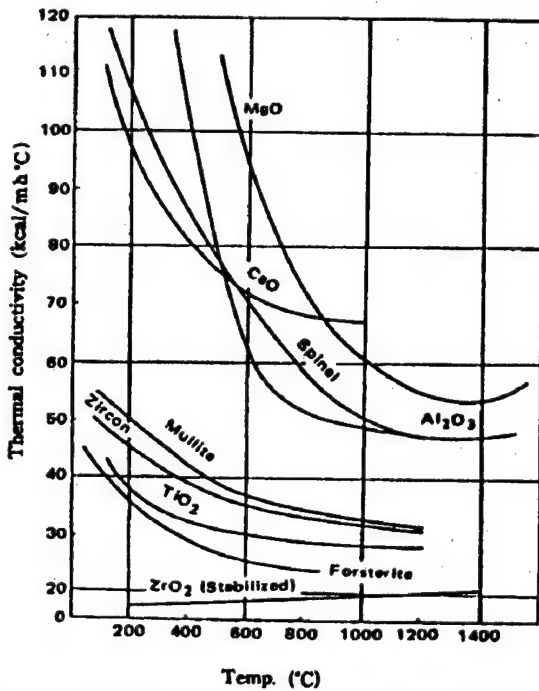


Figure 1. Thermal Conductivity of Various Metal Oxides Containing No Porosity

With a zirconia fiber board lined, small heat capacity and superior adiabatic quality of the lining material enables energy to be saved and the cooling rate to be adjusted with ease.

Another characteristic of pure zirconia is that its crystal form changes from monoclinic to tetragonal at temperatures around 1100°C, when several percent rapid change in volume takes place, causing cracks, thereby leading to its own fracture. To prevent this change in volume, several to 10-odd percent yttria, calcia, and magnesia are added to zirconia as stabilizers, heat treatment is provided, and zirconia is made into tetragonal and cubic forms to be stabilized. Stabilized zirconia comes to show virtually linear thermal expansion, resulting in no change in volume in the neighborhood of 1100°C. The additives used for its stabilization dissolve in zirconia with the result that lattice defects of oxygen ions are created in the crystal lattice, resulting in a conductor for oxygen ions.

This ion conductivity of zirconia is shown with those of other oxides in Figure 3. The drawing shows that electrical conductivity increases as temperature rises. Other characteristics of zirconia include small specific heat compared to other oxides, chemical stability, and superior corrosion resistance against molten metals and glass.

### 3. Applications of Zirconia

Attempts are being made for practical use of zirconia in many fields and its applied development using its various characteristics. Examples are presented below.

#### 3.1 Applications of Zirconia's Heat Resistance, Adiabatic Quality, and Corrosion Resistance

An example of these applications is a refractory, which has long been used as a lining material for glass and molten quartz kilns and for important sections

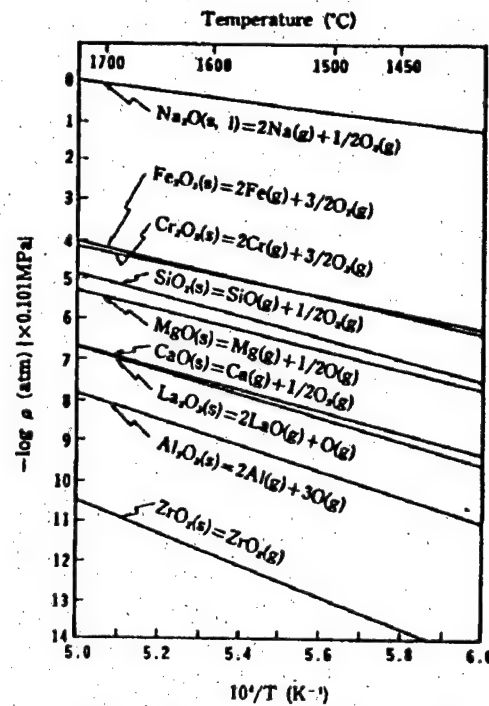


Figure 2. Vapor Pressures of Various Metal Oxides

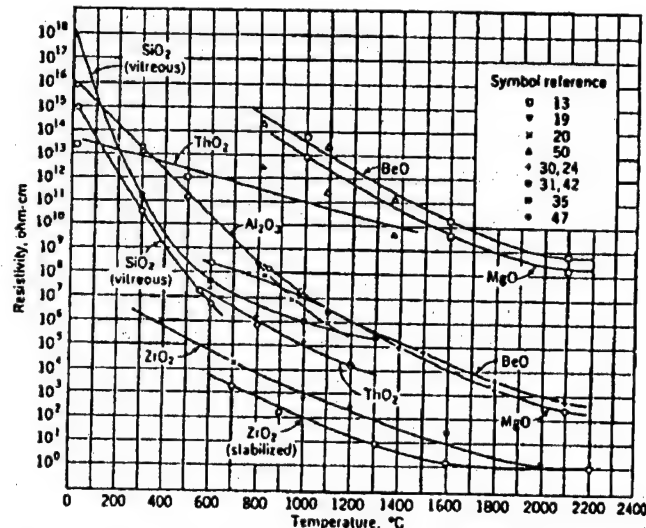


Figure 3. Electrical Resistivity of Refractory Oxides

in iron and steel manufacturing. A (tandish) nozzle used for steel manufacturing, an important refractory on which flow characteristics of billets and blooms depend, requires characteristics to prevent enlargement of a nozzle bore diameter and nozzle clogging, for which zirconia refractories are exclusively used. Also, zirconia is used in crucibles for melting metals, particularly of platinum, palladium, and rhodium.

Applications of zirconia using its heat resistance and adiabatic quality include a lining material for high-temperature kilns, and is important as an adiabatic material for ultrahigh temperature kilns using the heating element to be stated later. Furthermore, it is a material indispensable as a setter and a member for sintering electronic parts.

### 3.2 Applications of Ion Conductivity

Zirconia has long been applied as a refractory, but applications using its ion conductivity have been available fairly recently with some put to practical use, so that it can be said that these applications are still in a developmental stage. Their concrete examples include an oxygen sensor for oximeters, exhaust gas sensor for automobiles, oxygen sensor in metals, oxygen pumps, incomplete combustion sensor, solid electrolytic fuel cell, and steam cracking. A large number of books have been written on these examples, so brief descriptions of their principles will be provided here.

Figure 4 illustrates the basic principle of an oxygen sensor and an oxygen pump. When there exists the difference in oxygen concentration on either side of zirconia, oxygen ion migration from the high to low sides takes place to generate an electromotive force. This electromotive force is generated according to the following Nernst's equation, which when one oxygen partial pressure is known, provides the other oxygen partial pressure from an electromotive force generated.

$$E = \frac{RT}{4F} \ln \frac{P_c}{P_a} \quad (3.1)$$

where R, T, F,  $P_c$ , and  $P_a$  represent gas constant, absolute temperature, Faraday constant, and oxygen partial pressures of a cathode and an anode, respectively.

This phenomenon is the base of various oxygen sensors and adding a voltage to flow a current enables oxygen to be forcibly transferred, thereby permitting the sensors to actuate as oxygen pumps.

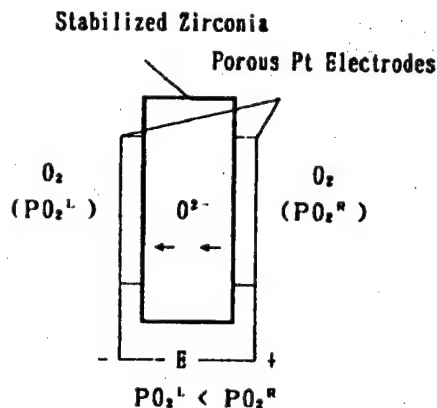


Figure 4. Schematic Diagram of Oxygen Ion Migration Through a Stabilized Zirconia Electrolyte

Figure 5 illustrates the principle of a solid electrolytic fuel cell. The basic principle is the same as that of an oxygen sensor. Future technology will apply the migration of oxygen ions in zirconia, with research into its practical use being promoted in many research institutes. Regarding fuels for this cell, the use of hydrocarbon gases, in addition to hydrogen shown in Figure 5, is being attempted, with hydrogen regarded as most promising when the generating efficiency and the influence of substances generated in reaction to the global environment are taken into consideration.

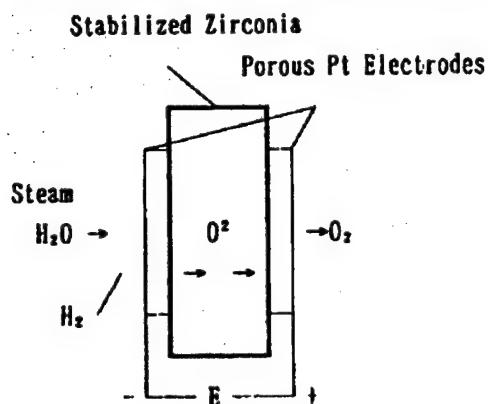


Figure 6. Fundamental Principle of the Electrolysis of Water Vapor

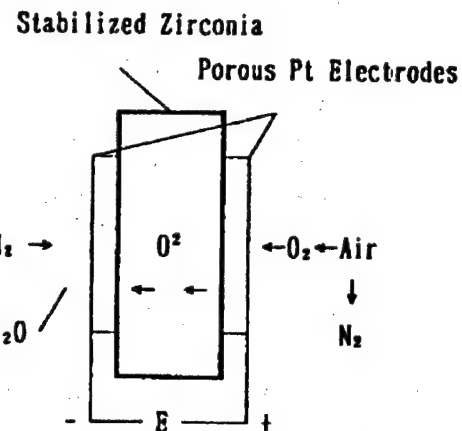


Figure 5. Fundamental Principle of a Zirconia Fuel Cell

Figure 6 shows a principle totally opposite that of the solid electrolytic fuel cell shown in Figure 5. When steam is supplied for zirconia to which a voltage is added to allow a current to flow, steam cracking occurs to allow only oxygen ions to pass zirconia, and hydrogen can be separated.

### 3.3 Applications of Conductivity

The applications applying conductivity generated by ion conductive ability include a zirconia heating element for resistance heating use.

A carbon heating element, enabling ultrahigh temperature heating to 2000°C in reducing and neutral atmospheres, has been put to practical use. In an oxidizing atmosphere, however, carbon undergoes oxidation dissipation and is unavailable. The development of zirconia has long been attempted as a heating element capable of heating up to 2000°C in an oxidizing atmosphere. Various studies on it have been reported, and at the same time themes and problems to be overcome, such as heat-resistant spalling quality and an arc-generating phenomenon, have been pointed out. The writer, et al., have succeeded in developing new zirconia that has overcome such problems, the description of which will be given later.

### 3.4 Applications of Toughness and Nonmagnetism

Applications of the mechanical property of zirconia include scissors, kitchen knives, and cutting tools. Cutting tools have proved useful in cutting various magnetic tapes because of their freedom from magnetism. This mechanical property results from the fact that when an external force is exerted on zirconia ceramics, its tetragonal crystal is dislocated to the monoclinic crystal and absorbs its energy.

#### 4. Zirconia Fiber

Considering that expanded applications of zirconia would require raw materials other than its powder, basic experiments were made on a fibrillation method and a crystal phase, thereby developing four types of fibers: nonstabilized zirconia fiber, calcia partially stabilized zirconia fiber, yttria partially stabilized zirconia, and magnesia-added zirconia fiber.

The following are descriptions of a method for fibrillation, basic experimental results on changes in a crystal phase in a developmental stage, and properties of the four types of fibers.

##### 4.1 Fibrillation of Zirconia and Crystal Phase Change in Fiber Precursor

Zirconia, a ceramic material with a melting point as high as about 2700°C, cannot be manufactured by a solution spinning method for general alumina-silica ceramic fibers involving melting alumina and silica raw materials by arc heat, etc., and their fibrillation by blowing. To cope with this, their fibrillation was carried out with the method shown in Figure 7. In other words, liquid composites such as calcia, yttria, and magnesia used as stabilizers and an organic binder are added to a solution obtained by specially denaturing and concentrating zirconium salt solution capable of forming zirconia by sintering to be mixed. The mixed solution undergoes cold spinning and a fiber precursor is formed. Then it is sintered to obtain a fiber.

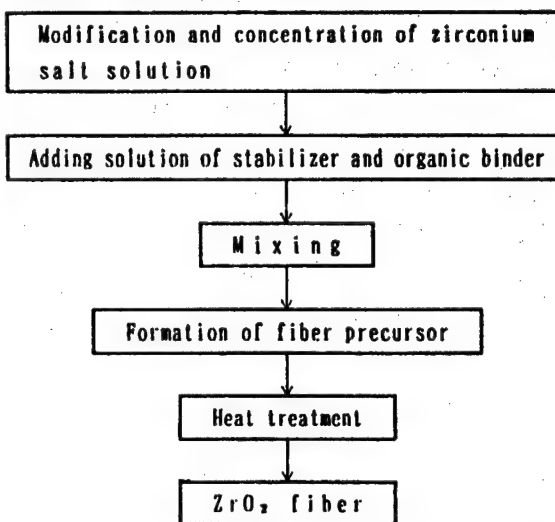


Figure 7. The Producing Process of ZrO<sub>2</sub> Fiber

While a change in the crystal phase of a zirconia fiber precursor is an important theme in manufacturing zirconia fibers by sintering a fiber precursor formed by the above method, basic experiments on sintering temperature and a change in the crystal phase were carried out repeatedly. As a result, a correlation between the crystal phase of a zirconia fiber precursor and its sintering temperatures shown in Figures 5 to 8 could be grasped, where the volume percentage of cubic zirconia was obtained by X-ray analysis of fiber precursors sintered at various temperatures and by calculating volume percentage of the cubic crystal from a diffraction chart.

$$Vt(\%) = \frac{T_{111}}{M_{111} + M_{111} + T_{111}} \times 100$$

where Vt represents volume percentages of cubic zirconia. T<sub>111</sub>, M<sub>111</sub>, and M<sub>111</sub> represent crystal surface diffraction peak integrated intensity of cubic

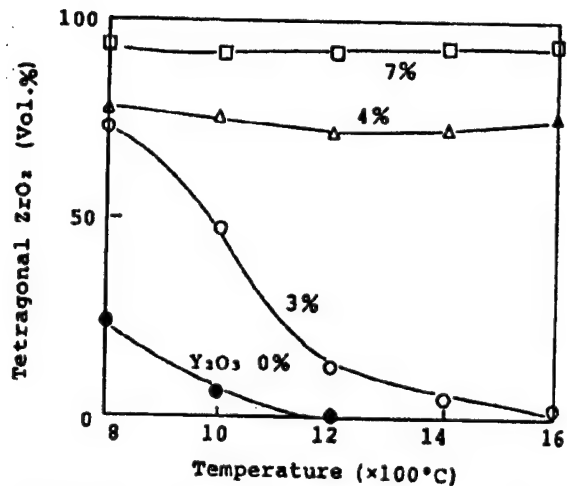


Figure 8. Phase Transformation of Zirconia Fiber Precursor Containing  $\text{Y}_2\text{O}_3$

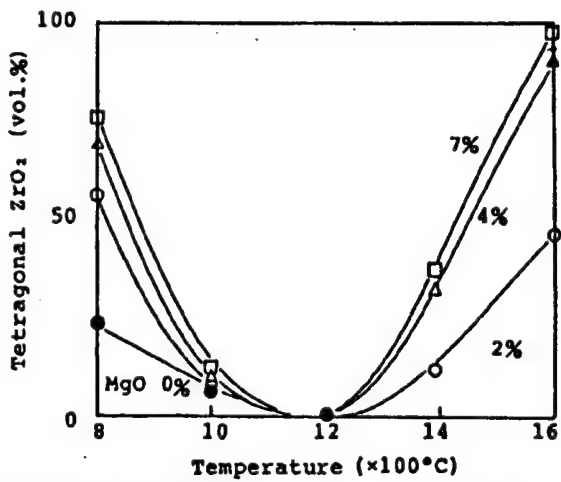


Figure 9. Phase Transformation of Zirconia Fiber Precursor Containing  $\text{MgO}$

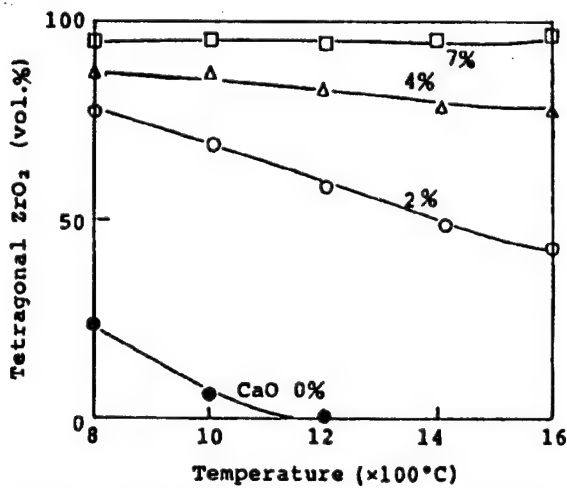


Figure 10. Phase Transformation of Zirconia Fiber Precursor Containing  $\text{CaO}$

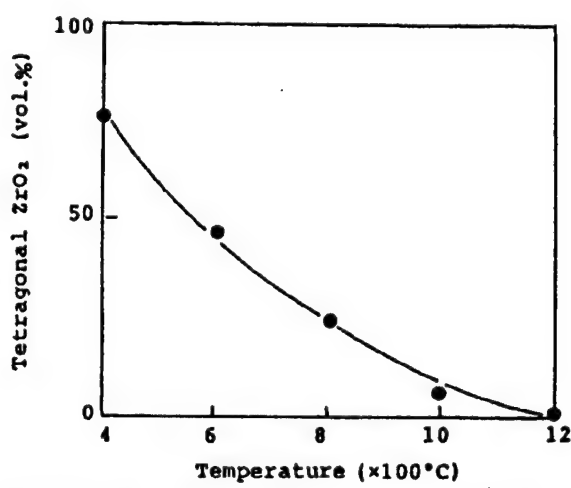


Figure 11. Phase Transformation of Zirconia Fiber Precursor Without Stabilizer

zirconia [111], rhombic zirconia [111], and rhombic zirconia [111], respectively.

As can be seen from Figure 11, the cubic volume percentage of a fiber precursor not containing a stabilizer decreases with sintering temperature, and a virtually perfect monoclinic crystal can be obtained at 1200°C. Figures 8 and 10 show changes in a crystal period of precursors of a calcia-contained zirconia fiber and a yttria-contained zirconia fiber, where with the amount of a stabilizer of over 4 percent, the cubic volume percentage is virtually constant. Figure 9 illustrates a change in the crystal phase of a magnesia-contained zirconia fiber precursor, showing that the cubic volume percentage

decreases with temperature until it reaches 1200°C and increases again after that.

#### 4.2 Representative Properties of Zirconia Fiber

The above basic investigation on crystal phases and the development of fiber manufacturing technology have enabled four types of zirconia fibers to be developed: nonstabilized fiber, calcia partially stabilized fiber, yttria partially stabilized fiber, and magnesia-added fiber. Figure 12 [not reproduced] shows a scanning electron microscopic photograph of a yttria partially stabilized zirconia fiber. It is a fiber with a flat surface about 5  $\mu\text{m}$  in size, the size of crystal particles composing the fiber being about 0.1  $\mu\text{m}$ .

The other three types show virtually similar appearances. Both a zirconia raw material and a stabilizer prepared by mixing in a solution, are distributed extremely homogeneously.

Table 1. Properties of Zirconia Fiber

Codes Properties	NZ	C4Z	Y7Z	M7Z
Chemical (%) composition	ZrO <sub>2</sub> +HfO <sub>2</sub> 99 CaO 4	ZrO <sub>2</sub> +HfO <sub>2</sub> 95 Y <sub>2</sub> O <sub>3</sub> 7	ZrO <sub>2</sub> +HfO <sub>2</sub> 92 MgO 7	ZrO <sub>2</sub> +HfO <sub>2</sub> 92 MgO 7
Crystal phase	Monoclinic	Tetragonal	Tetragonal	Monoclinic
Appearance		White		
Fiber diameter		Average 5 $\mu\text{m}$		
Fiber length	Average 0.5~3 mm		Average 20~30 mm	
Melting point		ca. 2600°C		
True specific gravity		5.8		
Thermal conductivity of Y7Z (kcal/h·m·°C) (W/m·°C)	500°C 1000°C 1500°C	0.10 (0.12) 0.26 (0.30) 0.75 (0.87)	0.12 (0.14) 0.17 (0.20) 0.23 (0.27)	When packed with a bulk density of 0.1 When packed with a bulk density of 0.4
	Remarks			

Table 1 shows types of zirconia fibers and their standard characteristic values. The four types of fibers can be used by selecting them according to their applications. A zirconia 100-percent nonstabilized fiber could be manufactured as it was found that it maintained a fiber form, although abnormal change in volume occurred due to crystal structural dislocation of zirconia's monoclinic and cubic crystals during final sintering in the fiber manufacturing processes. The average size of the four types of zirconia fibers is about 5  $\mu\text{m}$ , while the average fiber length of the nonstabilized fiber is 0.5~3 mm and that of the rest 20~30 mm. Their melting point is about 2600°C.

### 5. Zirconia Heating Element

It is known that a crystal stabilizer-added  $\text{ZrO}_2$  compact forms lattice defects of oxygen ions to be a conductor for oxygen ions at high temperatures. For this reason, it is used as a conductive solid electrolyte for oxygen sensors and in other fields. Attempts to apply a  $\text{ZrO}_2$  compact as a high-temperature heating element by heating it through energization have long been carried out, various studies have been reported, and themes and problems to overcome, such as creep deformation and heat-resistant spalling quality, have been pointed out.

The development of a zirconia heating element has been tackled from the standpoint that a heating element capable of heating to an ultrahigh temperature of about 2000°C in an oxygen atmosphere is indispensable for promoting the development and evaluation of ultrahigh temperature materials. The following are descriptions focusing on evaluation results of a new zirconia heating element that has recently been developed successfully, involving energization exothermic tests, electric resistance measurement, and changes in properties before and after energization exothermic.

Table 2. Typical Properties of the Zirconia Form

Chemical composition	(%)	$\text{ZrO}_2+\text{HfO}_2$ $\text{Y}_2\text{O}_3$	91 8
Bulk density		4.3	
Apparent porosity	(%)	27	
Modulus of rupture	(kgf/cm <sup>2</sup> ), (MPa)	550, (54)	
Crushing strength	(kgf/cm <sup>2</sup> ), (MPa)	900, (88)	
Specific heat	(kcal/kg°C), (J/kg°C)	0.21 (880) at 2000°C	
Thermal conductivity	(kcal/hm°C), (W/m°C)	0.60 (0.70) at 1500°C	
Thermal expansion	(%)	1.47 at 1500°C	

Table 2 shows typical properties of zirconia compact applicable as a heating element, and all the experimental results stated below are obtained using this material.

## 5.1 Measurement of Electric Resistance

### 5.1.1 Measurement of resistance by a two-probe DC method

A measuring specimen, a 10-mm diameter, 100-mm long cylindrical  $\text{ZrO}_2$  compact at either end of which a platinum wire was bound, was prepared. The specimen was placed in an electric furnace, and when the scheduled temperatures (1200-1550°C) were reached, a voltage of 1-5 V was applied on the platinum wire leading outside of the furnace, and a resistance was measured with two ordinary DC probes. Prior to this measurement, the difference between the four-probe and the two-probe method was examined with the result that virtually equivalent results were obtained, thus leading to the introduction of the latter. To prevent a fault current in refractories when a specimen was placed on them, the experiment was conducted with the specimen hung by a platinum wire.

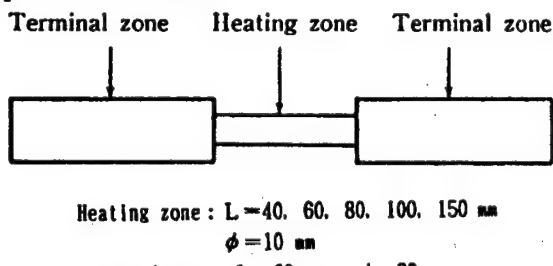


Figure 13. Schematic Diagram of the Zirconia Form as a Heating Element

The results are shown with continuous lines in Figures 13 and 14. Figure 14 shows the resistance value of Figure 13 by logarithmically plotting it, which indicates a linear relationship with temperatures. When this straight line is extended, the resistance value at 2000°C is estimated to be about 1  $\Omega\text{m}$ .

### 5.1.2 Calculation of resistance values by energized heating test

Several types of bar  $\text{ZrO}_2$  compacts varying in length of their heating parts alone were produced, and energization-use heating elements with a platinum rhodium wire installed in their probes were prepared. Figure 11 and Figure 12 [not reproduced] show their appearance and outlines of their contours and dimensions.

The thin white pipes installed at either end of the heating element shown in Figure 11 are  $\text{MgO}$  protective pipes that are intended to prevent vaporization of a platinum rhodium wire used as a lead wire. This heating compact was installed in a box of a  $\text{ZrO}_2$  insulator,  $\text{MoSi}_2$  heating elements were arranged outside of the box, and a  $\text{ZrO}_2$  compact was preheated with the external heating elements ( $\text{MoSi}_2$  heating elements) to 1500°C at a temperature-up rate of 7.5 °C/min. The  $\text{ZrO}_2$  compact, when 1500°C was reached, was energized to be heated

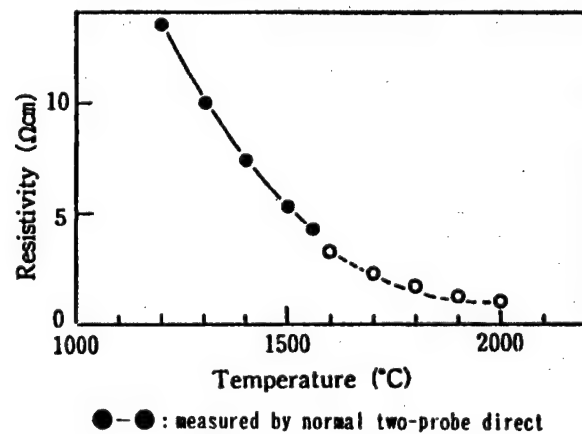


Figure 14. Resistivity of the Zirconia Form

●—●: measured by normal two-probe direct current method.  
○—○: calculated value from the data of the voltage and current of the zirconia form heated by flowing current.

Figure 14. Resistivity of the Zirconia Form

to 1600°C, 1700°C, 1800°C, 1900°C, and 2000°C at a temperature-up rate of 4.2 °C/min and cooled to ordinary temperature at the same rate after being retained at the predetermined temperature for two hours. In this energized heating test, current and voltage values impressed on the compact were recorded and the resistance value of the ZrO<sub>2</sub> compact with each temperature was calculated using expression (1).

$$R(\Omega \text{cm}) = (R_1 - R_2) \times \frac{S}{L_1 - L_2} \quad (1)$$

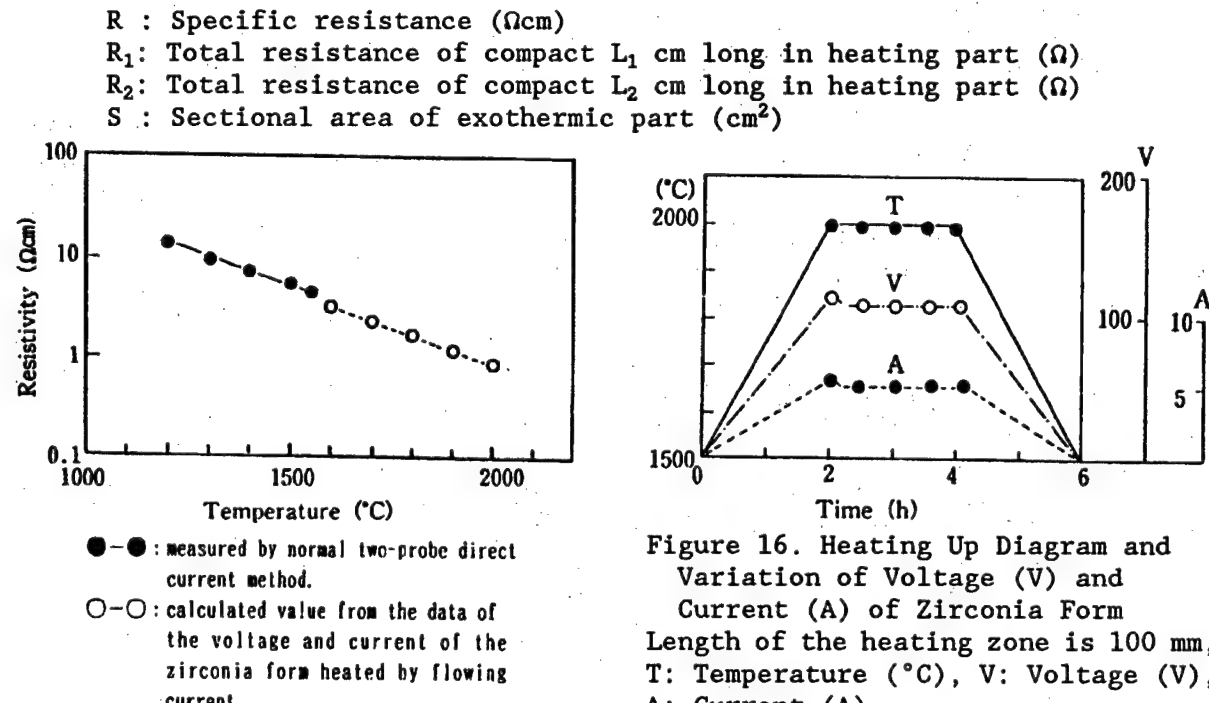


Figure 15. Logarithmic Plot of Resistivity of the Zirconia Form

Figure 15 shows the result of an energized heating test. The broken lines in Figures 13 and 14 show average resistance values calculated on the results of an energizing test of compacts that differ in heating part length. In the drawings, the values show a tendency to virtually agree with an extension of the result by the direct current method shown by continuous lines, while at 2000°C they were as small as about 10 percent. This difference seems to result from the difference in temperature at the external surface and the interior, since temperature was measured at the external surface of the heating

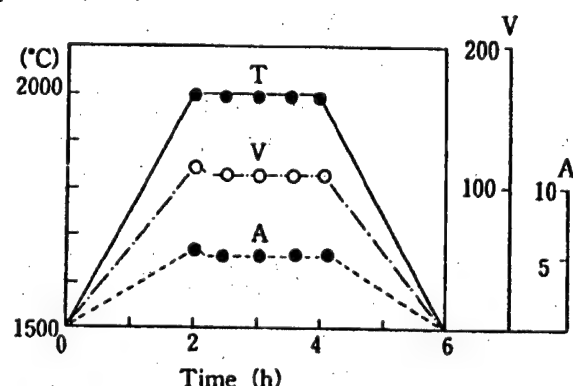


Figure 16. Heating Up Diagram and Variation of Voltage (V) and Current (A) of Zirconia Form  
 Length of the heating zone is 100 mm,  
 T: Temperature (°C), V: Voltage (V),  
 A: Current (A)

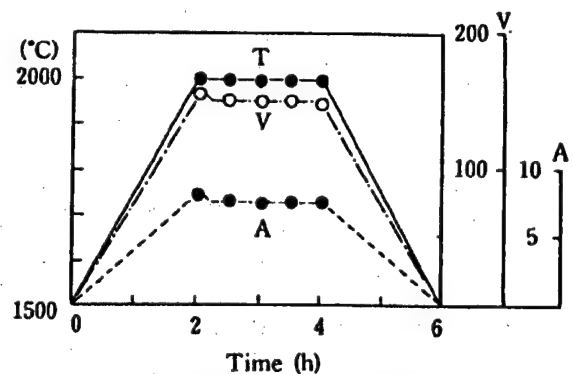


Figure 17. Heating Up Diagram and Variation of Voltage and Current of Each Zirconia Form in the Case of Heating 6 Zirconia Forms Simultaneously (Heating zone length: 100 mm)

part of the compact. In this context, a heating test at 2000°C similar to the previous one was conducted by incorporating six compacts 100 mm long in their heating parts. The results are shown in Figure 17. It was found that while compacts in Figures 17 and 16 were the same in shape, electric energy required to heat six compacts was about 50 percent. The resistance value calculated from the result of Figure 17 was about 1  $\Omega$ cm, agreeing with the value estimated from the result by the direct current method. This phenomenon seems to result from the fact that allowing compacts installed in parallel to heat up causes the temperature gradient of the specimen interior to diminish, thus making the surface temperature represent the inner temperature.

## 5.2 Property Changes Before and After Energized Heating Test

In order to examine property changes before and after an energized heating test of a  $ZrO_2$  compact, a change in the crystal phase was measured using an X-ray diffraction chart, a chemical analysis was made by the fluorescence X-ray bead method, and a change in its density was measured before being energized and after undergoing 50 repeated energized heating tests at 2000°C. The rate of the crystal phase calculated from X-ray diffraction was found from Garrie's literature expression, while the crystallite size was found from Scherrer's expression.

As for a change in resistance value, an important property of a heating element, a furnace incorporating six compacts 40 mm long with heating parts was constructed, 50 repeated tests at 2000°C under the above-mentioned temperature up/down conditions and a 500-hour continuous energized test was conducted, and a change in resistance value was examined.

(1)  $ZrO_2$  crystal phase: Figure 18 and Table 3 show an X-ray diffraction chart before and after the energized heating test and  $ZrO_2$  crystal phase and calculation results of crystallite sizes, respectively. It was found that about 10 vol% monoclinic crystal existed in a pre-energized  $ZrO_2$  compact, while the post-energized specimen was completely stabilized with no monoclinic crystal  $ZrO_2$  in it. The early feared destabilization phenomenon resulting from the displacement and vaporization of a stabilizer was not observed, with little increase in crystallite size.

(2) Chemical components and density: Table 4 shows chemical composition of a zirconia compact before and after energized heating. Although little change is observed in chemical components of  $ZrO_2$  and  $Y_2O_3$ , its main components, it is clear that  $Na_2O$  and  $Fe_2O_3$ , trace components, have diminished. As for a feared destabilization phenomenon when heating to a high

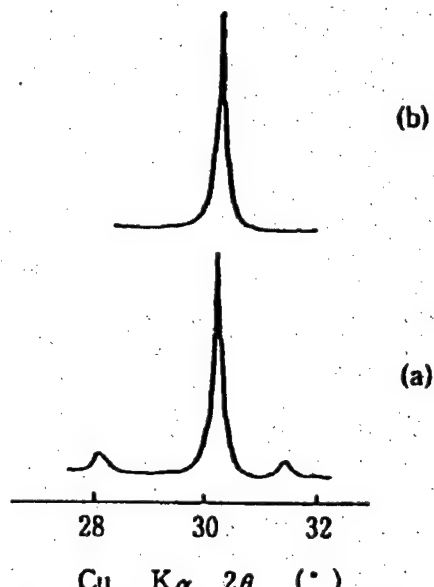


Figure 18. X-Ray Diffraction Patterns of the Zirconia Form  
 (a) Original;  
 (b) After heating

Table 3. Crystal Phase of Zirconia Form Before and After Heating Test

	Crystal phase	Crystallite size
Original zirconia form	Monoclinic $ZrO_2$ : 90 vol% Tetragonal : 10 vol%	380 Å
Zirconia form after heating test (Room temp. $\leftrightarrow$ 2000°C)	Tetragonal : 100 vol%	400 Å

Table 4. Chemical Composition of Zirconia Form Before and After Heating Test

	Chemical composition (%)						
	$ZrO_2$ + $HfO_2$	$Y_2O_3$	CaO	$Al_2O_3$	$SiO_2$	$Na_2O$	$Fe_2O_3$
Original zirconia form	91	7.9	0.1	0.2	0.7	0.1	0.2
Zirconia form after heating test (Room temp. $\leftrightarrow$ 2000°C)	91	7.9	0.1	0.2	0.7	0.0	0.0

Table 5. Density Change of Zirconia Form Before and After Heating Test

	Original zirconia form	After heating test
Dimensional change (%)	—	-2.0
Gravity change (%)	—	-0.3
Bulk density	4.3	4.5
Apparent porosity (%)	27	25

temperature of 200°C, the stability of the compact could be verified by chemical analysis. Table 5 shows density change before and after energized heating. The table shows about a 2 percent decrease in apparent porosity and about an 0.2 percent increase in bulk density, which are far from a sign of becoming closer in density, indicating little texture change.

(3) Resistance change: Figure 19 shows resistance change before and after 50 repeated heating tests at 2000°C. Figure 20 shows resistance change before and after a 500-hour continuous heating test. The resistance value after repeating the test 50 times increases by about 15 percent compared to the one for the

first test, while the value after 500 hours increases by about 5 percent compared to the early one. An increase in resistance during intermittent operation greater than that during continuous operation seems to result from structural microchange in a heating element because of heat history.

The possibility of applying a  $ZrO_2$  compact to a high-temperature heating element was evaluated and considered with the result that the following items have been made clear:

- (1) It has been proved that its electric resistance, an important property as a heating element, decreases with temperature and that it is about  $1\Omega$  at  $2000^\circ C$ ;
- (2) It has been confirmed that a  $ZrO_2$  compact shows little property change before and after energized heating, so that it is likely to be stably used for a long term.

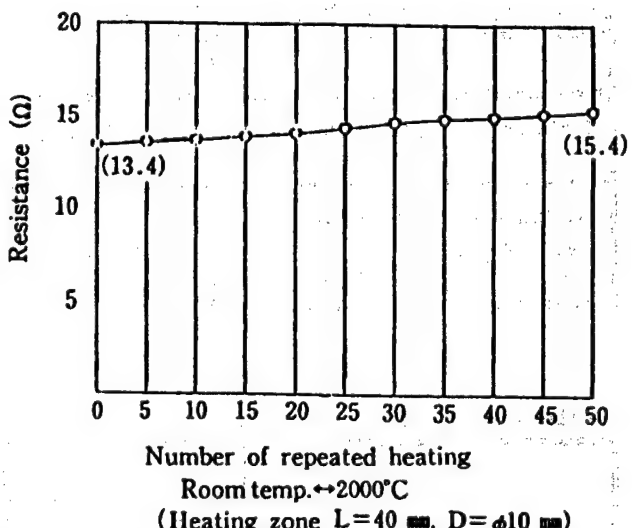


Figure 19. Electric Resistance Variation of the Zirconia Form in Repeated Heating

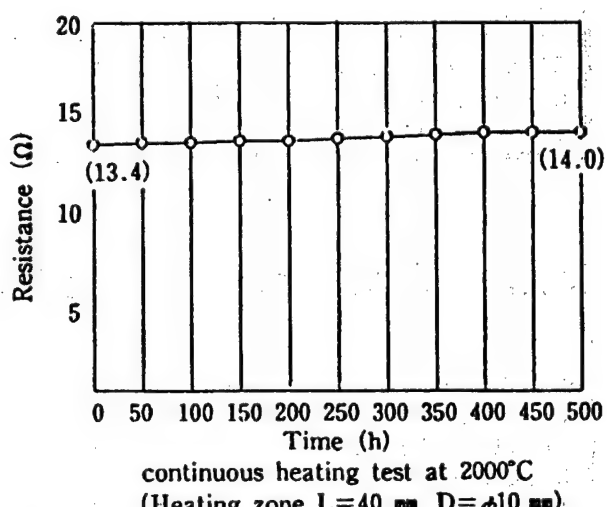


Figure 20. Electric Resistance Variation of the Zirconia Form in Continuous Heating

## **Plasmas, Related High-Temperature Materials**

926C0064C Ube CHO KO' ON ZAIRYO SYMPOSIUM in Japanese 12-13 Mar 92 pp 53-59

[Article by Osamu Fukumasa, Department of Electrical and Electronic Engineering, Faculty of Engineering, Yamaguchi University: "Thermal Plasma Processing and High Melting Point Materials; Nuclear Fusion Plasmas and Ultrahigh Temperature Materials"]

[Excerpts] **Abstract:** The purpose of this article is to identify plasmas with ultrahigh temperature materials. To this end, "thermal plasma processing" and "fusion plasmas" are extensively discussed. The former is discussed from the viewpoint of processing ultrahigh temperature materials, and the latter from the viewpoint of applying those to the first wall materials of fusion reactors.

### **3. Thermal Plasma Processing and High-Melting Point Materials**

One important advanced technology in recent years has been plasma processing. The technology involves precisely controlling intense reactivity of electrons, ions, and radicals in plasmas, applied to creating materials and surface treatment. As part of plasma applied engineering, the author, et al., are promoting research into establishing methods for producing and controlling low-temperature plasmas to thermal ones and their applications to plasma processing technology. The following are partial descriptions of their studies on thermal plasmas.

#### **3.1 Development of Thermal Plasma Processing System**

With respect to thermal plasma processing using plasma jet, producing ultrafine particles, spray coating and diamond synthesis of high-melting point materials are considered. Their purpose is to achieve large-capacity, homogeneous processing, a feature of low-temperature plasmas, using a plasma jet under reduced pressure while maintaining a high reaction rate, an advantage of thermal plasmas. The important themes to achieve this goal are the following:

(a) The development of a plasma source to stably supply a required plasma in a wide range of pressures and a reactor capable of injecting a processing substance into a high-temperature plasma flow and effective processing; and

(b) Precision measurement in terms of process control of particle density, temperature and rate of a plasma flow, and clarification such as heat transfer of interaction between a plasma flow and a processing material (powder material, in particular).

With regard to (a), the author, et al., have proposed and considered a processing system with feed rings for material feeding use connected to the front of the forced extension-type plasma jet generator, as shown in Figure 2. As a result, the processing system has the following features: (i) an arc column constrained by the insulated constrictor nozzle and its fixed length enables a stable jet with high thermal output to be produced under atmospheric to low pressure (several Torr); and (ii) Feed rings installed on the downstream side of the anode enables a powder material and a reactive material gas to be fed without any ill effect on arc discharge and generating jet.

### 3.2 Recent Research Examples

The following are brief descriptions of results of research recently conducted by the author, et al., on producing ultrafine particles of high-melting point materials using the processing system shown in Figure 2.

Figure 3 [not reproduced] shows scanning electron microscope (SEM) photographs of ultrafine particles before processing and those collected after a raw material was fed into a plasma flow. For materials, powder raw materials with an average grain size of  $20 \mu$ , such as  $\text{Al}_2\text{O}_3$  (melting point,  $2040^\circ\text{C}$ ),  $\text{TiC}$  melting point,  $3140^\circ\text{C}$ ), and  $\text{ZrC}$  (melting point,  $3570^\circ\text{C}$ ), are used. It was found that a large number of ultrafine particles (I.D., below  $0.1 \mu$ ) have been produced with vessel pressures of both 760 and 100 Torr. From these SEM photographs was found the number of particles (particle density) per unit area ( $0.1 \times 0.1 \text{ mm}^2$ ) and its grain size distribution was examined with the result that the grain size of about 99 percent of the number of particles collected was below  $0.1 \mu$ . Considering melting points and grain sizes of these materials, it was considered that injected powder materials successfully penetrated into the high temperature area of a plasma flow, undergoing melting

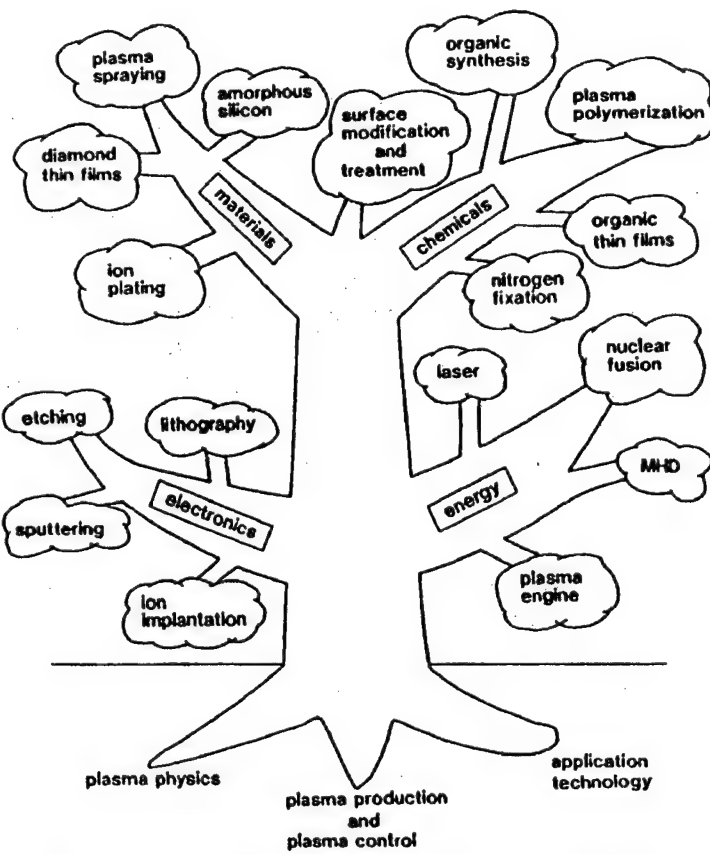


Figure 1. Application Fields of Plasmas

and vaporization. While their yields are currently under consideration, it was found that the use of this system enables high melting point materials to be refined even under reduced pressure.

Figure 4 shows the difference of a change in the feed ring length on the production of ultrafine particles. In these drawings, the relationship between the distance from the feed ring exit to the particle collecting point and the particle density of ultrafine particles of produced particles collected are shown. While the feed ring length increases with FR1, FR2, and FR3 in that order, experimental results show that the particle density of ultrafine particles collected increases with the feed ring length. In other words, acting as an effective area mixed with material particles and a plasma flow, field rings are expected to enable efficient thermal energy transfer to material particles.

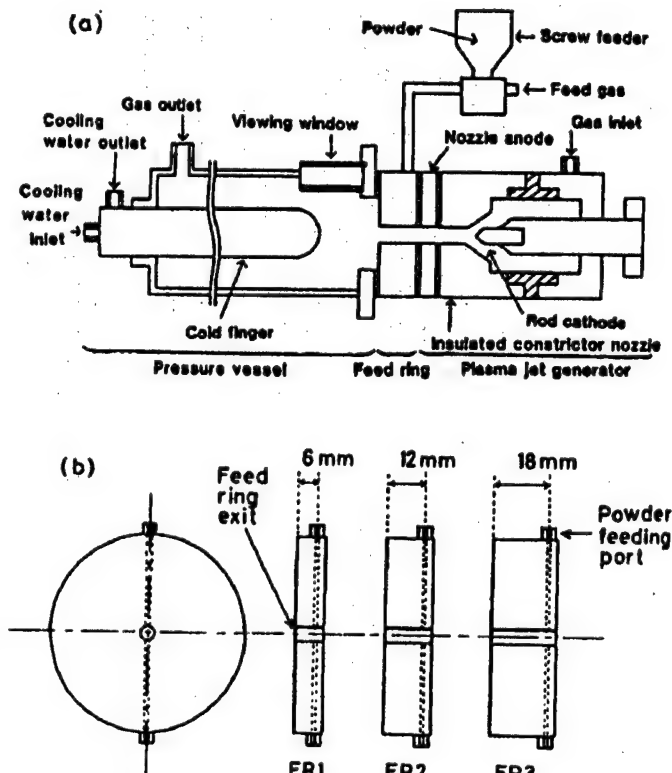


Figure 2. (a) Schematic Diagram of the Plasma Jet Reactor System, and (b) Three Feed Rings Used in the Experiment

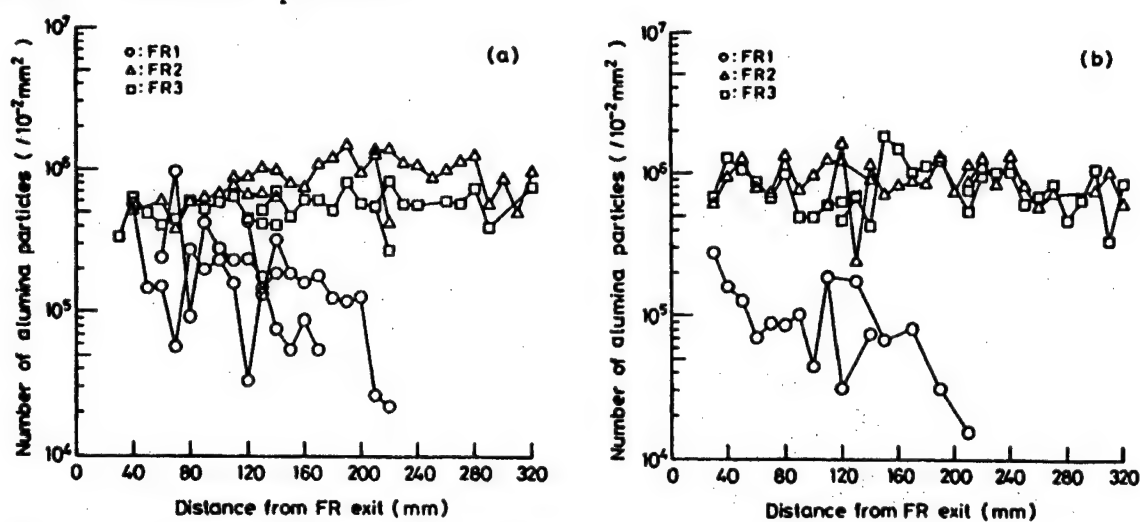


Figure 4. Density of Collected  $\text{Al}_2\text{O}_3$  Fine Particles (diameter:  $D \leq 0.1 \mu\text{m}$ ) Vs. Distance From the Feed Ring Exit  
(The particles are collected at (a) 760 Torr and at (b) 100 Torr.)

Control of the heating process for powder materials is important for processes using plasma jet. While it involves analysis using a single particle model, loci and temperature history of injected particles in a plasma flow are computed and the influence of vessel pressure on heating particles is being considered.

In other words, 1) under atmospheric pressure, particles are rapidly heated with their temperature history large depending on their grain sizes; 2) Knudsen effect being great under low pressure, particles are difficult to heat, most of them heated up to or close to their melting points with little difference in temperature history resulting from grain sizes; and 3) under low pressure, particles can fly at high speed even at locations distant from feed rings.

The above results indicate that particles are difficult to heat in general under low pressure. However, since high quality and large capacity in processing require producing particles and spray coating to be conducted under low pressure, the heat transfer amount under low pressure must be increased. Conceivable methods to this end are 1) increased temperature of a plasma flow, 2) extension of residence time of powder materials, and 3) increased heat transfer rates. With 1), it is possible to increase arc input effectively by extending the insulated constrictor section of a plasma jet generator. As for 2) and 3), it seems to be possible to increase the heat transfer amount by extending the axial length of feed rings and thereby expanding the high temperature/density area of a plasma flow. The above experimental results qualitatively correspond well to this.

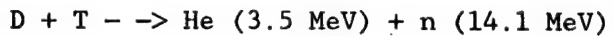
With diamond synthesis as a concrete example, a study is also being promoted on large capacity and homogenization of thermal plasma processing and a high-speed film forming method.

#### 4. Nuclear Fusion Plasma and Ultrahigh Temperature Materials

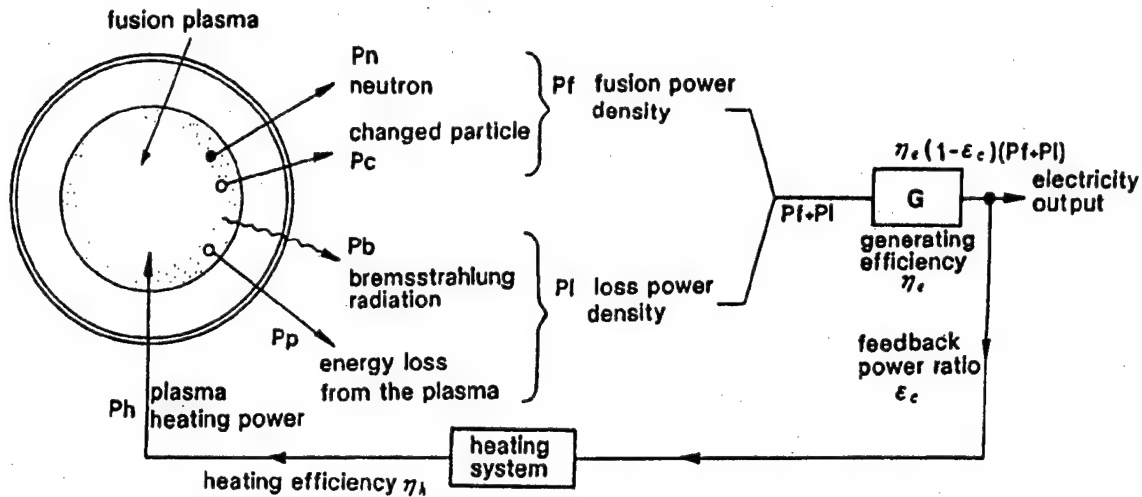
Nuclear fusion in the energy field is catching attention most as a plasma utilization method. It was the latter half of the 1950s that controller thermonuclear fusion began to be studied under the names of "clean energy" or the "sun over the earth." Then on 9 November 1991, JET succeeded for the first time in the world in obtaining thermal output of 1.8 MW by D-T nuclear fusion reaction. As a core for nuclear fusion is of an ultrahigh temperature plasma, confining this ultrahigh temperature plasma relates to ultrahigh temperature materials exposed under severe service conditions. The following are general descriptions.

##### 4.1 Conditions for Core Plasma

In terms of an energy source, D-D, D-T, and D-<sup>3</sup>He reactions are considered in reality as nuclear fusion reactions to meet such conditions that sources are profound and economically obtainable and that reaction is easy to occur (sectional area of reaction is large). Of them, D-T reaction is under R&D, which can be expressed as



where He and n represent helium and neutron, respectively. The figures in parentheses of reaction products in the right side represent energy of the respective particles, the sum of which is total energy discharged by nuclear fusion reaction. MeV, a unit of generated energy, is mega electron volt (1 MeV =  $10^6$  eV; 1 eV =  $1.6 \times 10^{-10}$  J).



steady state  $\rightarrow P_l = P_h$

$$\text{fusion power amplification factor } Q = \frac{P_f}{P_h} = \frac{P_f}{P_l}$$

$$\text{overall efficiency } \eta = \frac{P_h}{P_f + P_l} = \frac{1}{Q + 1} = \epsilon_c \eta_e \eta_h$$

Figure 5. Schematic Diagram of Power Flows in a Steady-State Magnetic Fusion Reactor

For a nuclear fusion reactor to function as an effective energy source, there is a requirement for an ultrahigh temperature plasma to be its core. Power balance in a reactor system will be considered here assuming a magnetic field confinement system for a steady-state operation reactor. Figure 5 illustrates a power flow on a nuclear fusion reactor system. Nuclear fusion reaction power  $P_f$  is a sum of neutron output  $P_n$  and charged particle (ion) power  $P_c$ . Also, plasma causes an electronic braking radiation loss of  $P_b$  and a thermal energy loss of  $P_p$  in the form of plasma particle, resulting in a total power loss of  $P_l$ .  $P_f$  and  $P_l$  are recovered and converted into electric energy. Part of this electric power is used for heating a plasma, and heating input  $P_h$  is thrown into the plasma via the heating system.

A nuclear fusion reactor operating in a steady state maintains an equilibrium state by refilling as much heating energy as energy lost by a plasma; hence,  $P_l = P_h$ . Lawson has given a condition using  $\eta$ , a product of generating efficiency of thermal energy and plasma heating efficiency, that heating input  $P_h$  necessary for keeping a plasma to meet the condition of a nuclear fusion

reactor for its power balance is below a factor  $P$  ( $\eta < 1$ ) of total output from a plasma containing nuclear fusion reaction. Lawson criterion can be expressed as

$$P_n = P_b + P_1 \leq \eta (P_f + P_b + P_1)$$

The individual terms of the above equation can be described using plasma density  $n$ , ion temperature  $T_i$ , and energy confinement time  $\tau$ , and the condition for  $\eta = 1/3$  is called Lawson criterion. Lawson criterion is sometimes called a critical core plasma condition or a zero power condition. Under this condition, when  $T_i = 10$  keV (about 100 million degrees),  $n_i \geq 10^{14} \text{ cm}^{-3} \cdot \text{s}$  is obtained with D-T reaction, which is the target value of research on heating and confinement of plasmas in large-size tokamaks (JET, JT-60, and TFTR).

#### 4.2 Configuration and Functions of Nuclear Fusion Reactor

Figure 6 illustrates the configuration of a magnetic field confinement system D-T nuclear fusion reactor. Its core is an ultrahigh temperature plasma with  $T_i$  of hundreds of millions of degrees, comprising equivalents of D and T. The plasma is confined in the core by a magnetic field so as not to come into contact with the reactor wall. He ions generated as a result of reaction are also confined by the magnetic field with D and T. Having no charge, neutrons are free to move and collide against the reactor wall, but with energy as high as 14.1 MeV, plunge into the outside blanket through the reactor wall.

D and T, a fuel in a core plasma, and He, its ash, depart the confinement area by diffusion based on a time constant corresponding to their individual confinement time, and eventually disappear. Therefore, in order to keep constant densities of D and T in a plasma, it is necessary to refill a fuel. He atoms (alpha particles), a reaction product, confined in a magnetic field with as high an energy as 3.5 MeV, collide against a cold fuel refilled to give it energy, thereby rendering it useful for heating a new fuel. This is called alpha particle heating, which diminishes plasma heating energy needed to be injected from an external energy source, thus contributing to the profitability of a reactor, serving as a base for achieving self-ignition (plasma combustion without input).

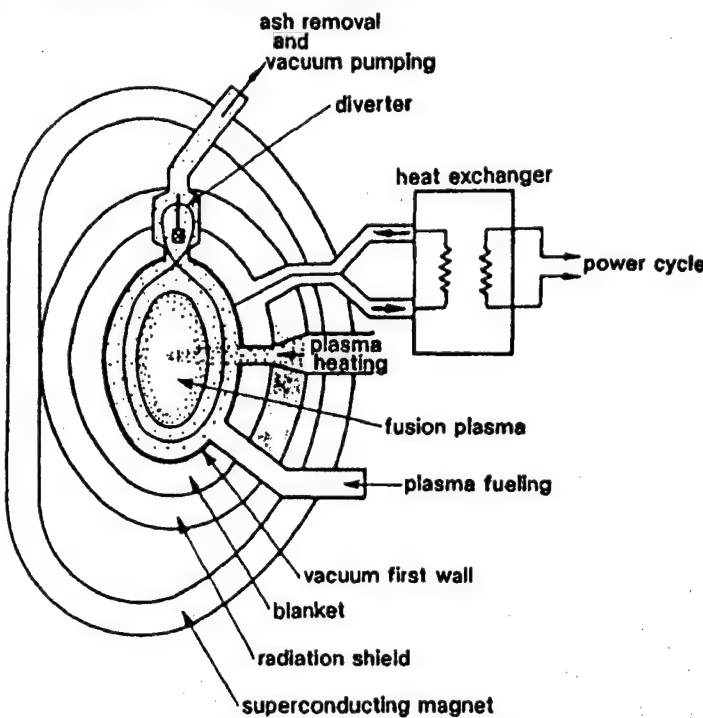


Figure 6. Schematic View of Components for Fusion Reactors

Of the structural materials of a nuclear fusion reactor, the part facing a plasma is called the first wall. The first wall is irradiated by electromagnetic waves (X- and  $\gamma$ -rays) and high-energy particles (D, T, He atom ions, impurity atom ions in plasmas, and neutrons). Incident energy into the first wall per unit area per unit time is called wall load. How to select this wall load is very important for conceptual design of a nuclear fusion reactor, on whose value the size of a reactor (and its power density) depend. As hazardous irradiation damage is realized, lower values have come to be employed, with ones as low as  $2-4 \text{ MW/m}^2$  often used recently. There is a section called blanket outside of the first wall, functions of which are to decelerate neutrons, produce T, a fuel (breeding) of tritium and discharging heat from the reactor (cooling).

In the outermost part of the reactor is arranged a superconductive magnet, which generates a magnetic field for confining a plasma. To prevent leak of neutrons from the blanket, a radiation shield layer is arranged between the blanket and the superconductive magnet.

## 5. Conclusion

In this article, general descriptions of 1) the thermal plasma process and 2) ultrahigh temperature nuclear fusion plasma that are expected to make progress in the future have been presented with some examples of research done by the author, et al., in terms of the relationship between plasmas and ultrahigh temperature materials. The authors' will be pleased if the descriptions, although incomplete, help readers understand engineering applications of plasmas. They will also be pleased if the readers take interest in the themes selected concerning fields to be tackled from now on.

Additionally, with reference to item 1) above, the understanding of thermal plasma properties under intermediate pressures (one to tens of Torr) and the development of production and control methods are desired, as well as further R&D for producing and controlling ultrahigh temperature plasmas with respect to item 2). Yet these are desired not irrespective of materials (development). For example, the plasma-opposed equipment (the first wall's divertor) taken up in item 2) needs the improvement of a material itself to use a high atomic number metal like W; however, it is more imperative to make a plasma (particularly an end plasma) suitable for introducing W. What is troublesome, or interesting, with R&D for plasma-opposed materials is that when a plasma condition changes, so does a suitable material. In this respect the same applies to item 1) in a reverse sense. In other words, there is a choice of a process or an object (material to be produced) suitable for a system (plasma) or a system suitable for the object, and here again, it is necessary to develop control technology for a wide range of plasmas.

## Some Problems of Technology Advanced Structural Materials Testing, Evaluation at Ultrahigh Temperature

926C0064A Ube CHO KO' ON ZAIRYO SYMPOSIUM in Japanese 12-13 Mar 92 pp 81-90

[Article by Kazumi Hirano, Mechanical Engineering Laboratory, Agency of Industrial Science and Technology, MITI: "Trend in R&D for Advanced Structural Materials; Fracture Dynamic Evaluation and Research; Themes of R&D for Evaluation Testing Technology; Plan of Actual Environmental Evaluation Testing"]

[Text] **Abstract:** R&D on technology for advanced materials testing and evaluation is one of the most important and urgent problems for the progress of a high-performance structural materials project. In this paper, the current status of R&D activities for advanced structural materials in Japan is outlined. Next, a few current research projects, especially fracture mechanics of advanced composite materials relating to evaluation of the damage tolerance behavior, are generally introduced. Some technical problems are also discussed to research and develop the materials testing and evaluation methods at an ultrahigh temperature. Finally, the outline of HIPMEX (high-performance materials experiment), which MITI proposes as one mission for the recovery-type capsule program (EXPRESS) between Japan and Germany, is introduced from the viewpoint of the materials test under the actual reentry environment (high temperature, high pressure, and oxidizing atmosphere).

### [Text] 1. Introduction

R&D for advanced materials as key technologies to support advanced technologies has become increasingly active, covering a wide range. In the aerospace field, for example, R&D for advanced materials from new metals to composite materials aimed at multifunctionalization of materials and hazardous environmental resistance is actively promoted. Lightweight high-strength materials superior in ultrahigh heat resistance and thermal protective quality, in particular, are likely to control developmental planning involving aerospace, thus positioned as the most important material (Figure 1).

On the other hand, success in R&D for advanced materials, mechanical and structural, depends upon how to maintain strength/toughness and strength/durability at the same time. The importance of their durability is also

beginning to be realized along with full-scale R&D for advanced materials and their increased maturity, or in terms of their assured long-term reliability and expanded applications. Considering their application to primary structural members of aerospace equipment, in particular, in terms of their assured structural soundness under ultrahigh temperatures, the evaluation of damage admissibility

seems to be an important and urgent research theme. Furthermore, in relation to this, the importance of actual environmental evaluation testing including ground dummy actual environmental testing has increasingly been brought into focus. However, R&D for technology for evaluation and testing of properties of structural materials in the ultrahigh temperature area, led by basic dynamic property, has just begun with numerous developmental themes.

In this article, an outlook on R&D for new metals and inorganic advanced structural materials will be provided through descriptions of Japan's few national projects currently underway to which the author is related, concerning advanced structural materials. Here, using examples of recent research on fracture dynamic evaluation, descriptions will be provided of a problem of strength concerning the evaluation of damage admissibility that is important not only in property evaluation but material design, process technology development and its practical use, and research themes involving evaluation and testing, including actual environmental evaluation and testing. Finally, a brief description of the "HIPMEX" project, will be given, as well as actual environmental evaluation and testing of heat-resistant materials used for reentry of a capsule related to the Japanese-German joint "Recovery Capsule" project, the so-called EXPRESS project.

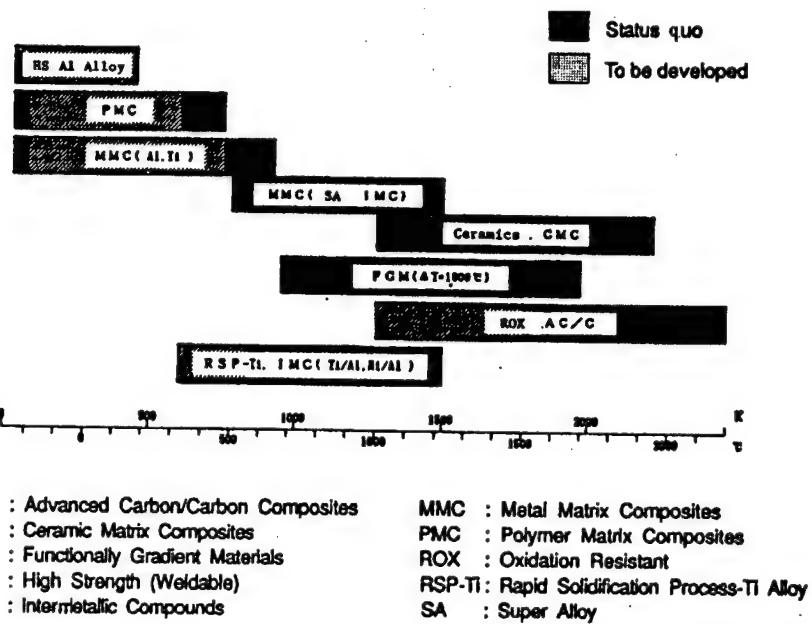


Figure 1. Temperature Capability of Advanced Structural Materials in the Field of Aeronautics and Aerospace Technologies

## 2. Trend of R&D for Advanced Structural Materials

### 2.1 National Projects

Japan's national projects related to R&D for advanced structural materials include the ones by the Next-Generation Industrial Key Technologies R&D System of the Agency of Industrial Science and Technology [AIST], MITI, and by the Expenses for Promotion of Science and Technology of the Science and Technology Agency. In the "Composite Material" project of the AIST, R&D for polymeric and metallic composite materials had been promoted until 1988, followed by the "Ultrahigh Environment-Resistant Advanced Material" project over eight years beginning in 1989. R&D is actively under way with the cooperation of the government, private sector, and academia for intermetallic compounds, composite materials with intermetallic compounds as matrixes, and carbon/carbon composite materials including acid-resistant coating. For details, refer to report by Sakamoto. The "Fine Ceramics" project has been under way for a decade. It is also planned to promote the "Ultrahigh Reliability Inorganic Fusion Material" project aimed at supplementing defects of ceramics and a combination of structure (material) and function (material) by high-order microstructural control.

In the "Functionally Gradient Material" project based on a new material design concept developed in Japan, the development of new continuous texture-controlled ceramics/metal and ceramics/ceramics materials superior in ultrahigh heat resistance and thermal protective quality has been under way on a five-year program since FY 1987.

### 2.2 Developmental Targets and Prediction of Performance Improvement

Figure 2 shows present values of structural materials and very low-temperature tank materials of a space plane in the relationship between specific strength and temperature and expected values of improved performance of medium- and long-term developmental targets of the above national projects. For a concept of space plane, material performance values of at least 1.3 times those at present are necessary with both structural and tank materials (indicated by slanting lines in the drawing).

With polymeric composite materials, materials with sufficient target performance values have been obtained, the important research themes for which are the improvement of heat and acid resistance in resins and carbon fibers to achieve the mid- and long-term target of 725 K.

With metallic composite materials the mid-term target values are likely to be virtually achieved by the development of an  $\text{SiC}_{\text{CVD}}/\text{RSP-Ti}$  alloy composite material. Also, at 1300 K, the long-term target service temperature, composite materials of intermetallic compounds such as TiAl can be said to be the most promising candidate material.

With alloys, both an RSP-Ti alloy and titanium intermetallic compounds have strengths close to the mid-term target values expected to be achieved if progress is made in the development. The key to their practical use will

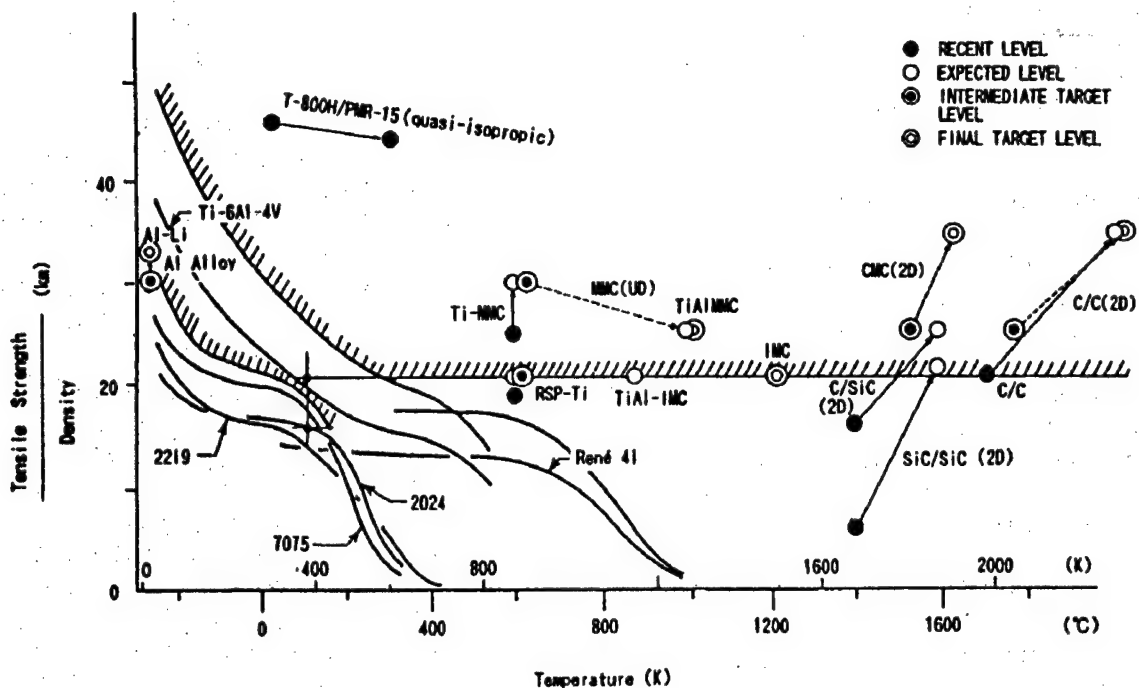


Figure 2. Goal for Specific Strength of Structural and Engine Materials for Space Planes

rather be the development of secondary processing technology. The long-term target values are to be achieved by the development of high-melting point intermetallic compounds, such as niobium and molybdenum, both of which are in a stage of basic research, necessitating the development of a manufacturing process including forming workability in the future.

While candidate materials in the ultrahigh temperature area exceeding 1500 K are ceramics and ceramics compound materials (CMCs), the developmental target values of single ceramics are set to considerably high levels for a structural material, compared to present and expected values, with a large gap. This results from low tensile strength and toughness unique to ceramics, and to achieve these target values, it seems to be necessary to introduce innovative technologies, such as nanocomposite materials and whisker-reinforced composite materials proposed for the basic research stage.

Long fiber-reinforced CMCs is the most promising as a heat-resistant structural material, already put to practical use in the forms of carbon fiber/SiC and SiC fiber/SiC. With two-dimensional reinforced materials, their values are expected to reach the target value levels of structural materials; to this end, however, heat resistance of present ceramics fibers represented by an SiC fiber must be improved. To achieve the long-term target values, it is necessary to improve properties in three-dimensional reinforced structure and important to achieve the fiber developmental target values by improving performance of heat-resistant ceramics fibers.

Close to the mid-term target values in terms of strength, C/C composite materials are very likely to achieve the long-term target values from their expected values. The greatest developmental theme is how to solve oxidation resistance, the key to which is the development of oxidation-resistant coating technology for composite materials and carbon fibers.

### **3. Research on Fracture Dynamic Evaluation**

Descriptions of research on fracture dynamic evaluation concerning the evaluation of damage allowability of advanced structural materials, such as metallic composite materials, intermetallic compounds, functionally gradient materials, and C/C composite materials, are omitted due to space limitations. Recent research by the author, et al., explanations, and research perspectives are provided in the bibliography [not reproduced]. The standardization for evaluation testing methods of metallic composite materials also related to this subject is actively under way, an international collaboration project being planned.

### **4. Themes of R&D for Evaluation Testing Technology**

#### **4.1 Themes Evaluation Testing Technology Under Ultrahigh Temperatures**

As can be seen with mid- and long-term developmental targets and expected values of improved performance, very extreme heat resistance is expected for advanced structural materials. However, with virtually no material property evaluation testing method established under ultrahigh temperatures exceeding 1500°C, it is urgent to develop and readjust evaluation testing technology including testing devices and instrumentation technology to ensure universality of property data and to enable comparison between data. This is important, in particular, not only to affect material development but to ensure material reliability and to expand material applications in the ultrahigh temperature area.

The themes of developing common basic technologies related to basic dynamic property evaluation include the following:

- (1) Development and readjustment of a testing unit for evaluating material properties under ultrahigh temperatures (including oxidizing atmosphere).
- (2) Development of rapid, highly efficient property evaluation testing technology using multiple microspecimens.
- (3) Development of measuring strain and monitoring technologies under ultrahigh temperatures.

## 4.2 Developed, Readjusted Testing Equipment for Evaluating Ultrahigh Temperature Materials

### (1) Ultrahigh temperature material testing equipment

Figure 3 [not reproduced] shows an example of evaluation equipment for material strength properties under ultrahigh temperatures. The example comprises a closed loop electrohydraulic material testing unit, an atmosphere-controlled ultrahigh temperature reactor, and an ultrahigh temperature displacement measuring unit. The equipment enables various fracture dynamic material tests to be conducted under ultrahigh temperatures of up to 2000°C in vacuum ( $10^{-5}$ Torr) and inert gases (argon and nitrogen).

### (2) Strain measurement technology under ultrahigh temperatures

Figure 4 shows a schematic diagram of strain measurement technology. A target such as a projection (using the difference in lightness from the back visual field under ultrahigh temperatures) is set on a specimen, and change in movement in the target caused by load is observed as an amount of movement of an object in the XY plane using a high-resolution CCD camera. Observation data are processed at high speed by an image processing computer and change between the center of gravity of the target and that of the target moved is measured as elongation. Measurement is conducted in a range between 0-10 mm with a resolution of 1  $\mu$ m at a sampling speed of 10 times/second. The use of this equipment enables macrodeformation and fracture behavior of a specimen to be observed directly by a monitoring television.

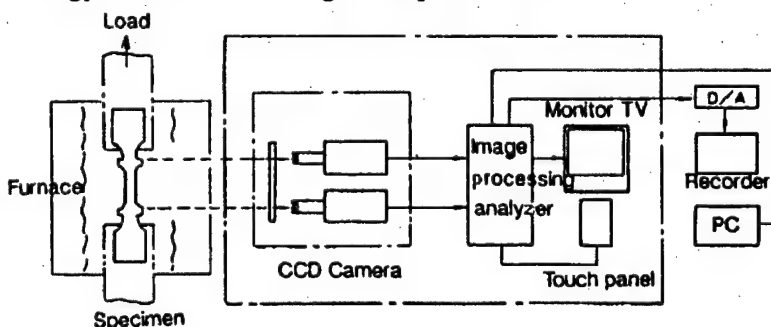


Figure 4. Schematic Illustrations of Strain Measurement Methodology

## 4.3 Integrated Evaluation Testing Method

It is important to integrate evaluation testing methods to ensure the universality of property data and enable mutual comparison between data. In the next-generation "Ultrahigh Environment-Resistant Advanced Material" project, the integration of evaluation testing methods is currently under way by the measurement technology committee in relation to the evaluation of mid-term target performance. The following are descriptions of a draft of an ultrahigh temperature tensile test method for C/C composite materials.

### (1) Applicability

This draft relates to the regulations on tensile testing methods under ultrahigh temperatures for multidimensional reinforced C/C composite materials developed in the next-generation project. The applicability does not apply to one-way reinforced materials.

## (2) Testing equipment

- Testing machine

The testing machine shall be one specified in JIS B 7721, which is capable of keeping testing speed constant. A closed-loop electrohydraulic material testing machine may be used.

- Testing jig

The testing jig shall be one that is capable of ensuring sufficient in-plane and out-of-plane alignment, and may be either pin load or collet chuck and either mechanical or hydraulic.

- Heating system (heating method)

The heating system shall be one that uses a heating furnace equipped with a temperature adjustment mechanism and is capable of heating uniformly and constantly in an allowable range of  $\pm 10$  K over the total range of the distance between the gauge marks of specimens during testing. Either a total heating system or a local heating system may be introduced provided it meets the above tolerance. With temperature measurement, either a thermocouple system or a noncontact one may be used provided it ensures that specimen temperature does not exceed the above temperature tolerance.

- Strain (displacement) measurement method

An extensometer for measuring tensile elastic modulus and fracture strain shall be in principle capable of measuring elongation of either side of a specimen with a precision of  $\pm 0.005$  mm or above. When using a noncontact displacement measuring device, such as a laser or a CCD camera, it shall be equivalent or superior to an extensometer in performance.

## (3) Specimens

- Contour and dimensions

Table 1. Dimensions of Standard Tensile Test Specimens

Parallel part length	Above specimen width x 5
Distance between gauge marks	$30 \pm 1$ mm
Width	$8 \pm 0.1$ mm
Thickness	2~3 mm

Specimens shall have uniform cross sections and parallel parts. Table 1 and Figure 5 show the contours and dimensions of a standard specimen.

For measuring strain using a noncontact displacement gauge, a target made of a C/C compound or high melting point metal is added to the parallel parts.

The thickness of a compact shall be used in principle; however, according to levels of strength, an adhesive tab capable of withstanding ultrahigh temperatures may be installed or thin walls uniform in a range of thickness specified in Table 1 may be introduced into parallel parts of specimens.

- Number of specimens

The number of specimens shall be five or above; however, data of those broken at other than the target points shall be invalid.

#### (4) Testing methods

- Heating methods

For heating, a temperature-up rate free from thermal shock or creep deformation shall be used, and after reaching the predetermined temperature until the initiation of a test, the test temperature shall be retained for over 10 minutes. Care should be taken to ensure that heating does not exceed the predetermined temperature.

- Test speed: A crosshead speed of 0.05-5 mm/min shall be used.

- Measurement:

- 1) Tensile load-strain diagrams in the fracture process shall be recorded in succession or properly at a virtually equal interval.
- 2) Maximum tensile load and maximum strain shall be recorded.

#### (5) Summary of test results

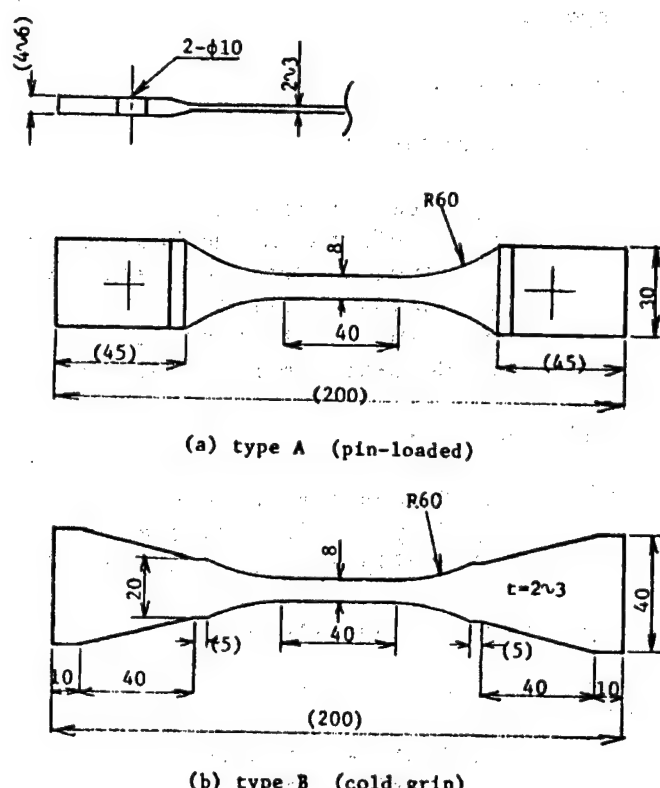


Figure 5. Drafts for Configuration and Dimensions of Standard Tensile Test Specimen

## (6) Reports

- Report items

- 1) Test materials

- a) Types of materials
- b) Manufacturing methods and conditions
- c) Manufacturers and manufacturing lot numbers
- d) Laminated structure
- e) Volume content of reinforced fiber
- f) Heat-treatment conditions

- 2) Specimens

- a) Processing methods
- b) Sampling locations and bearings
- c) Configurations and dimensions of specimens

- 3) Number of specimens

- 4) Test temperature

- a) Test temperature
- b) Heating method
- c) Average temperature-up rate
- d) Retention time

- 5) Test speed

- 6) Test results

- a) Tensile elastic modulus
- b) Tensile strength
- c) Fracture strain

- 7) Date of test

- Desirable subjunction items

- 1) Macro fracture state of specimens

- 2) Test results

- a) Typical tensile stress-strain diagram
- b) Poisson ratio
- c) Average values, standard deviation, and coefficient of variation of the above 6) items.

- 3) Other items believed necessary

As part of summarizing integrated performance evaluation items from the long-term standpoint, a plan for integrating various property evaluation and testing methods other than the ultrahigh temperature tensile test method is beginning to be promoted.

#### **4.4 Establishing Design Concepts of Equipment and Structures**

How to design equipment and structures superior in ultrahigh heat resistance and heat preventive quality by using characteristics of ultrahigh environmental resistant advanced materials rich in potential abilities, i.e., the establishment of so-called structural design concept, depends upon distinct evaluation standards of damage tolerance of advanced materials. In that sense, this design is closely related to R&D themes of evaluation and testing thermal conductivity.

R&D for the following themes is important and urgent: technology for evaluating fracture dynamic property, technologies for damage analysis and monitoring, technology for evaluating damage tolerance, and technology for nondestructive evaluation of life and complementary life. It is also necessary to establish an R&D support system reorganizing evaluation and testing organizations, including ground dummy real environment testing facilities, and structuring a database for material design through R&D for property evaluation technology.

### **5. Real Environment Evaluation and Testing Project**

#### **5.1 Necessity of Real Environment Evaluation and Testing**

As stated above, there are many research themes in developing evaluation and testing technologies of basic properties, environmental resistance and dummy real environments, and a system for evaluation and testing.

With ultrahigh environmental-resistant advanced materials led by C/C composite materials, on the other hand, the more advanced materials become, the more difficult it becomes to distinguish material design, working process, and property evaluation fields from one another. Therefore, it is necessary to carry out R&D, not in such a way as to regard them only as developing materials by removing borderlines of the three fields, but as part of equipment and structures. In other words, it must be considered from an overall standpoint, including material utilization technology. To this end, with respect to next-generation aerospace-use advanced structural materials, it is necessary to promote R&D aimed at overall performance, including actual environmental evaluation. Actual environmental evaluation tests must be conducted. Furthermore, learning basic technology for actual environmental evaluation tests seems to be necessary as part of R&D for advanced heat-resistant structural materials. Following is a brief summary of why actual environmental evaluation tests are needed:

##### **(1) Creation of flight (usable) real environment and ensuring it**

- For material performance evaluation under flight (usable) real environment and screening of candidate structural materials

(2) Comparison with and study of ground mockup environmental evaluation tests

- Definite positioning of ground mockup environmental evaluation tests and verification of its validity (study)
- Clarification of material damage mechanism under real environment
- Formulation of evaluation standards for damage tolerance under real environment
- Formulation of guidelines for material design

(3) R&D for ultrahigh heat-resistant structure design technology

(4) R&D for evaluation technology for structural soundness of ultrahigh heat-resistant structures.

- Structuring of basic concept for ensuring reuse-oriented structural soundness with respect to the above technology that depends on computer simulation
- Acquiring basic data for developing the above technology and its accumulation

(5) Development and reorganization of large-size ground (dummy real environment) test facilities and acquiring basic data for the same project

## 5.2 Actual Environmental Evaluation Tests Using Recovery-Type Capsule

As stated above, in next-generation aerospace development led by space planes, real environmental evaluation tests for candidate structural materials cannot be avoided. With real environmental evaluation tests using a re-entry capsule, it is difficult to make a total heating amount and heating time equivalent to those of a space plane, but by properly setting the ballistic coefficient and curvature of the aerodynamic heating surface of a re-entry capsule, the maximum aerodynamic heating ratio and its generating altitude can be set to values equivalent to those of a space plane. Therefore, it is considered that real environmental evaluation testing using a re-entry capsule has great importance.

(1) Significance (expectation)

Expectations for real environmental evaluation tests using a recovery capsule in terms of R&D for advanced ultrahigh heat-resistant structural materials include the following:

- 1) Implementation of performance evaluation and screening of ultrahigh heat-resistant structural materials under R&D in real environment
- 2) Implementation of R&D for ultrahigh heat-resistant structure design technology and learning of its basic techniques

3) Early initiation of R&D for structural soundness evaluation technology for ultrahigh heat-resistant structures

Therefore, for Japan, which has no recovery capsule technology, expectations for heat-resistant material experiment "HIPMEX" in the EXPRESS project (to be stated later) seem to be great.

(2) Requirements

Following are the requirements for the total program of real environmental evaluation tests using a recovery capsule:

1) Heat-resistant structure design

- a) Structural design of advanced structural materials achieved in next-generation project R&D focusing on C/C composite materials for mounting and recovering them on and from a capsule
- b) Implementation of heat-resistant structure design for experimental location as part of recovery capsule design
- c) Implementation of optimum heat-resistant structure design supposing re-entry real environment
- d) Evaluation of structural soundness by computer simulation

2) Instrumentation and evaluation of real environment in capsule re-entry

- a) Environmental instrumentation of surface temperature and pressure distribution of a capsule in its re-entry
- b) Grasp of environmental conditions of experimental location
- c) Study of validity of computer simulation analysis

3) Evaluation testing after capsule recovery

- a) Evaluation of structural soundness of oxidation-resistant coating films:

—Evaluation of surface damage degree

- Surface analysis
- Sectional observation (including observation by electron microscope)
- State of generation and progress of thermal cracks
- State of separation of oxidation-resistant coating films (layer)
- Measuring of loss of oxidation-resistant coating films
- Grasp of ablation state, etc.

—Evaluation of residual strength

- Measuring of basic dynamic property
- Measuring of fracture dynamic property, etc.

b) Verification of validity of heat-resistant structure design

- Material used
- Structural form, etc.

4) Implementation of testing of ground dummy real environmental evaluation tests

- a) Measuring of basic thermal properties
- b) Measuring of basic dynamic properties
- c) Implementation of arc wind tunnel test

5) Comparison of results between real environmental evaluation tests and testing dummy real environmental evaluation tests

- a) Formulation of guidelines for material design of oxidation-resistant coating and process technology development
- b) Formulation of testing method for ground dummy real environment and basic study of its integration

6) Comprehensive evaluation

- a) Formulation of guidelines for material design of ultrahigh heat-resistant structural materials
- b) Orientation of R&D for design technology involving ultrahigh heat-resistant structures
- c) Structuring of basic concept for ensuring soundness of ultrahigh heat-resistant structure
- d) Proposals involving reorganization programs for large-sized ground research facilities

### 5.3 Recovery Capsule Development Project

A recovery capsule system is an unmanned space system involving launching a capsule by a rocket into a circumearth orbit, implementing mission during circumearth flights and allowing the capsule to come back to earth. This system has attracted attention recently as a powerful means of microgravity experiments for its capability of maintaining a fairly good microgravitational environment for a fairly long time. As an intergovernmental cooperation project based on the Japan-Germany Science and Technology Cooperation Agreement, R&D for a recovery-type capsule project, the so-called EXPRESS (Experiment Re-Entry Space System), was planned. Figure 6 and Table 2 show the

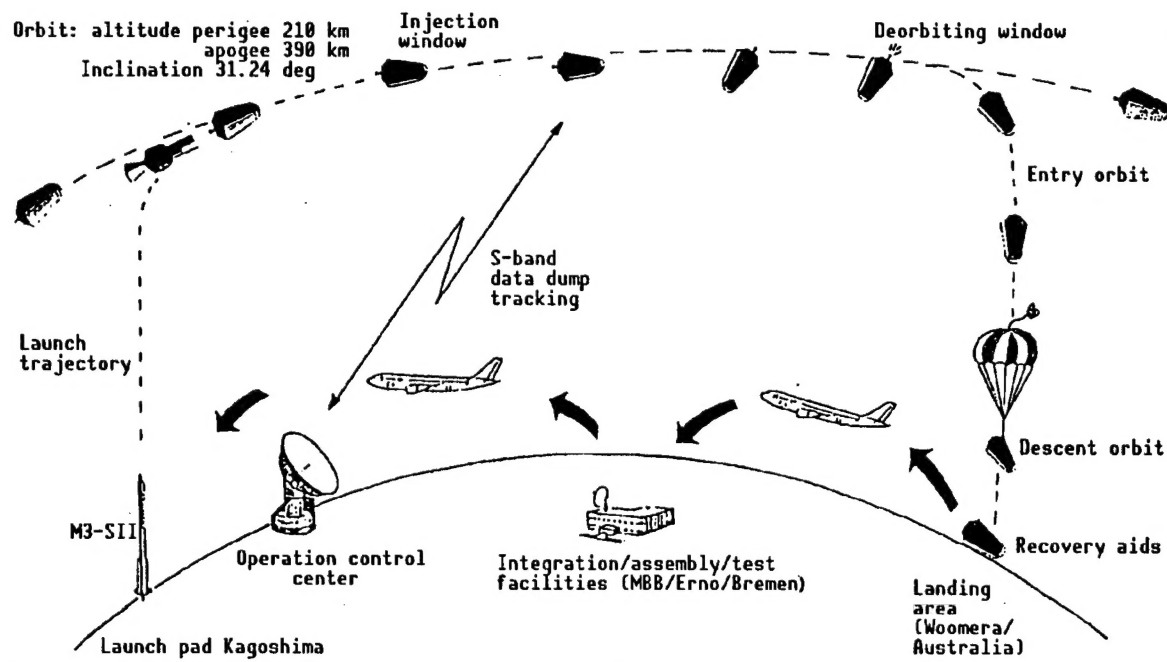


Figure 6. Plan for Recovery-Type Capsule Program (EXPRESS) Between Japan and Germany

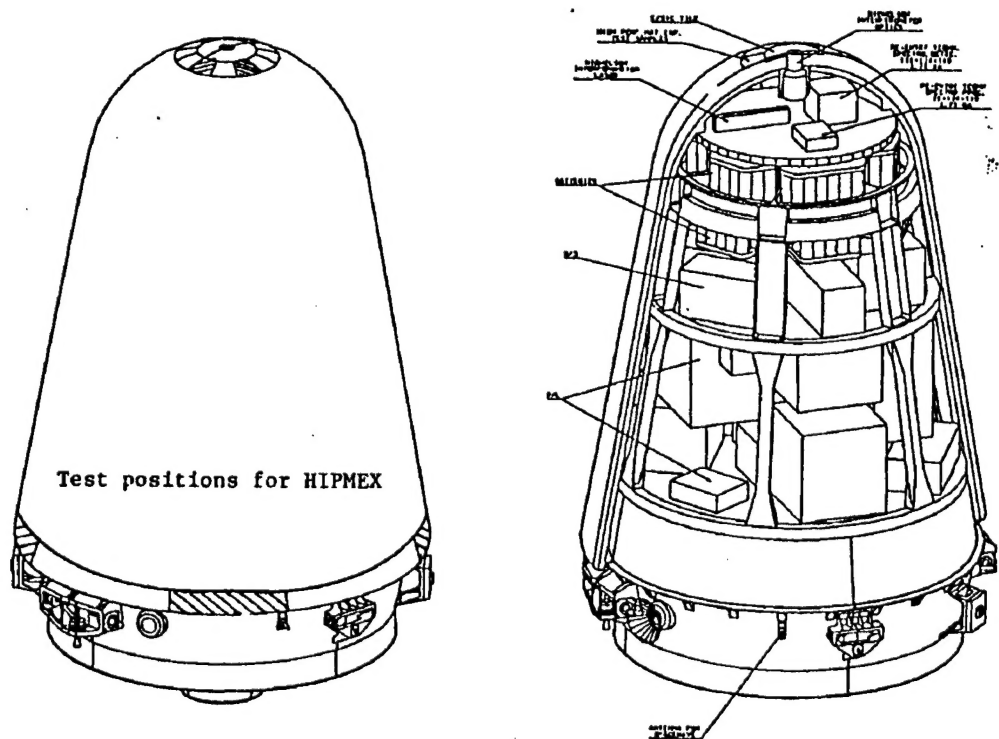


Figure 7. Outline of HIPMEX

Table 2. List of First Flight Mission (Draft)

Experimental field	Experimental theme	Experimental content	Abbreviation of theme	Nation in charge
Micro-gravity experiment-related field	Catalyst creation experiment	Creation of high-performance catalysts	CATEX	Japan
	TEM furnace experiment	Material evaluation by high temperature (1450°C) furnace	TEMFA	Germany
Re-entry experiment-related field	Environmental instrumentation experiment	Gas density measurement by lasers Measurement of temperature and pressure High-temperature measurement	Michelson Interferometer Free Flight Measurement Experiment PYREX	Germany
		Measurement of pressure distribution and aerodynamic heating distribution and emission spectra measurement	R-TEX	Japan
	Ablator performance evaluation	Heat-resistant material	(C/SiC tile)	—
		Heat-resistant material	(C/C tile)	HIPMEX
Sensor-related field	Induction sensor experiment	Evaluation of IMU and GPS performance	SPACENARV	Germany

operating program (proposal) for the mission of the same plan and the experimental mission (under planning) for the first flight. A high-performance materials experiment (HIPMEX) was proposed by the Japanese as heat-resistant materials experiments in atmospheric re-entry of a capsule. Committees were organized within the Unmanned Space Experimental System Research and Development Organization and Next-Generation Metals and Composite Materials Research and Development Association. Active formulation of the detailed program of the experiment is under way (Figure 7).

"OREX," a similar re-entry aerodynamic heating test not involving capsule recovery, is being planned in reaction to the HOPE project.

## 6. Conclusion

National projects related to a few advanced structural materials currently under way in Japan were picked up, and discussions were given on trends of R&D for new metals and nonorganic advanced materials focusing on the aerospace field and a problem of strength related to evaluation of damage tolerance with recent research examples. Also, the necessity and significance of the real environmental evaluation tests were discussed while taking up R&D themes concerning technology for evaluating properties in the ultrahigh temperature area. Furthermore, a project for real environmental evaluation tests using a recovery capsule was presented.

What is important in terms of practical use of advanced structural materials and their expanded applications includes formulation of guidelines for material design, the development and standardization of testing and evaluation technologies, and the development of design technology for equipment and structures using advanced materials.

## Acknowledgement

Research on fracture dynamic evaluation in this article is being carried out as part of the R&D for evaluation technology in the next-generation project. The author would like to thank the committees and those concerned for their cooperation in allowing him to refer to the investigation reports of the Japanese Aerospace Industry Association and the Space Plane Developmental Trend Investigation Committee in presenting section 2.

- END -

NTIS  
ATTN PROCESS 103

2

5285 PORT ROYAL RD  
SPRINGFIELD VA

22161

This is a U.S. Government publication. Its contents in no way represent the policies, views, or attitudes of the U.S. Government. Users of this publication may cite FBIS or JPRS provided they do so in a manner clearly identifying them as the secondary source.

Foreign Broadcast Information Service (FBIS) and Joint Publications Research Service (JPRS) publications contain political, military, economic, environmental, and sociological news, commentary, and other information, as well as scientific and technical data and reports. All information has been obtained from foreign radio and television broadcasts, news agency transmissions, newspapers, books, and periodicals. Items generally are processed from the first or best available sources. It should not be inferred that they have been disseminated only in the medium, in the language, or to the area indicated. Items from foreign language sources are translated; those from English-language sources are transcribed. Except for excluding certain diacritics, FBIS renders personal names and place-names in accordance with the romanization systems approved for U.S. Government publications by the U.S. Board of Geographic Names.

Headlines, editorial reports, and material enclosed in brackets [] are supplied by FBIS/JPRS. Processing indicators such as [Text] or [Excerpts] in the first line of each item indicate how the information was processed from the original. Unfamiliar names rendered phonetically are enclosed in parentheses. Words or names preceded by a question mark and enclosed in parentheses were not clear from the original source but have been supplied as appropriate to the context. Other unattributed parenthetical notes within the body of an item originate with the source. Times within items are as given by the source. Passages in boldface or italics are as published.

#### SUBSCRIPTION/PROCUREMENT INFORMATION

The FBIS DAILY REPORT contains current news and information and is published Monday through Friday in eight volumes: China, East Europe, Central Eurasia, East Asia, Near East & South Asia, Sub-Saharan Africa, Latin America, and West Europe. Supplements to the DAILY REPORTs may also be available periodically and will be distributed to regular DAILY REPORT subscribers. JPRS publications, which include approximately 50 regional, worldwide, and topical reports, generally contain less time-sensitive information and are published periodically.

Current DAILY REPORTs and JPRS publications are listed in *Government Reports Announcements* issued semimonthly by the National Technical Information Service (NTIS), 5285 Port Royal Road, Springfield, Virginia 22161 and the *Monthly Catalog of U.S. Government Publications* issued by the Superintendent of Documents, U.S. Government Printing Office, Washington, D.C. 20402.

The public may subscribe to either hardcover or microfiche versions of the DAILY REPORTs and JPRS publications through NTIS at the above address or by calling (703) 487-4630. Subscription rates will be

provided by NTIS upon request. Subscriptions are available outside the United States from NTIS or appointed foreign dealers. New subscribers should expect a 30-day delay in receipt of the first issue.

U.S. Government offices may obtain subscriptions to the DAILY REPORTs or JPRS publications (hardcover or microfiche) at no charge through their sponsoring organizations. For additional information or assistance, call FBIS, (202) 338-6735, or write to P.O. Box 2604, Washington, D.C. 20013. Department of Defense consumers are required to submit requests through appropriate command validation channels to DIA, RTS-2C, Washington, D.C. 20301. (Telephone: (202) 373-3771, Autovon: 243-3771.)

Back issues or single copies of the DAILY REPORTs and JPRS publications are not available. Both the DAILY REPORTs and the JPRS publications are on file for public reference at the Library of Congress and at many Federal Depository Libraries. Reference copies may also be seen at many public and university libraries throughout the United States.